
Electronic Thesis and Dissertation Repository

8-9-2018 2:30 PM

Hydrodynamics of a Gas-Driven Gas-Liquid-Solid Spouted Bed

Jia Meng, *The University of Western Ontario*


Supervisor: Jesse Zhu, *The University of Western Ontario*

Co-Supervisor: Dominic Pjontek, *The University of Western Ontario*

A thesis submitted in partial fulfillment of the requirements for the Master of Engineering
Science degree in Chemical and Biochemical Engineering

© Jia Meng 2018

Follow this and additional works at: <https://ir.lib.uwo.ca/etd>

 Part of the [Complex Fluids Commons](#), and the [Other Chemical Engineering Commons](#)

Recommended Citation

Meng, Jia, "Hydrodynamics of a Gas-Driven Gas-Liquid-Solid Spouted Bed" (2018). *Electronic Thesis and Dissertation Repository*. 5518.

<https://ir.lib.uwo.ca/etd/5518>

This Dissertation/Thesis is brought to you for free and open access by Scholarship@Western. It has been accepted for inclusion in Electronic Thesis and Dissertation Repository by an authorized administrator of Scholarship@Western. For more information, please contact wlsadmin@uwo.ca.

Abstract

A novel cylindrical gas-driven gas-liquid-solid spouted bed was developed in this project, which has a high potential to be used for a biological wastewater treatment process. Solids motion, flow regimes, and regime transitions in this system were studied. With increasing gas velocity, four regimes were identified, including: fixed bed, semi spouted bed, full spouted bed and internal circulating fluidized bed. The respective gas velocities for the transitions between the four regimes were experimentally identified and termed as minimum spouting velocity, full spouting velocity and minimum circulating velocity. A new “basketing” method was adopted to measure the minimum spouting velocity while the particle velocity and dense phase retraction in the annulus were monitored to determine the full spouting velocity and minimum circulating velocity. The effects of key operating parameters on the three transitional velocities were examined in this novel spouted bed. When a draft tube was present, these three velocities increased with increasing particle density and draft tube length. The minimum spouting velocity and full spouting velocity were not affected when varying the nozzle-tube gap, while the minimum circulating velocity increased with longer nozzle-tube gaps. Without a draft tube, the gas-driven gas-liquid-solid spouted bed stability is reduced, where results were mainly obtained in terms of the water level, initial static bed height and gas flowrate.

Keywords

Gas-driven gas-liquid-solid spouted bed, Hydrodynamics, Draft tube, Spouting velocities, Flow regimes

Co-Authorship Statement

Title: Hydrodynamics in Gas-driven Gas-liquid-solid Spouted Bed with Draft Tube

Author: Jia Meng, Jesse Zhu, Dominic Pjontek, Xinran Li

The experimental apparatus of gas-driven gas-liquid-solid spouted bed with draft tube was constructed by Jia Meng under guidance of the advisors. Jia Meng performed all the experiments and drafted this paper. Xinran Li provided useful assistance in some experiments. Data analyses and process were undertaken under the advice of Dr. Jesse Zhu and Dr. Dominic Pjontek. The final version of this paper is ready for submission

Title: Hydrodynamics in Gas-driven Gas-liquid-solid Spouted Bed without Draft Tube

Author: Jia Meng, Jesse Zhu, Dominic Pjontek

The experiment apparatus of gas-driven gas-liquid-solid spouted bed without draft tube was constructed by Jia Meng under guidance of the advisors. Jia Meng performed all the experiments and draft this paper. Data analysis and modification were undertaken with advice of Dr. Jesse Zhu and Dr. Dominic Pjontek.

Acknowledgments

I would like to express my sincerely appreciation to all people who have been supporting me and helping me in my academic and daily life.

My sincerely gratitude to Dr. Jesse Zhu for being my supervisor. Thanks to his motivation and supervision especially for giving me this opportunity to pursue my master study. His knowledge and enthusiasm not only stimulate me throughout the study, but also broaden my horizon for the years to come.

My heartfelt thanks to Dr. Dominic Pjontek for being my co-supervisor. His knowledge provided very good support to my thesis and help me solve my puzzles in this project. Thanks to his patience in helping me improving my English writing. It has been a pleasure to work with him.

Much appreciation to George Zhang and Tian Nan for their help in equipment construction and technician support.

Special thanks to Bowen Dreuw for his great help in proof-reading the final draft of my thesis.

Many thanks to my friends and group member for their advice and support.

Great gratitude to my parents for their selfless supports and for continuous encouragement.

Finally, I would like to express my heartfelt thanks to my girlfriend Tianzi Bai. I cannot insist without her encouragement and love.

Table of Contents

Abstract.....	i
Co-Authorship Statement.....	ii
Acknowledgments.....	iii
Table of Contents	iv
List of Tables	vii
List of Figures	viii
List of Appendices	x
Nomenclature	xi
Chapter 1	1
1 General Introduction	1
1.1 Background.....	1
1.2 Thesis objectives.....	8
1.3 Thesis structure	9
Reference	10
Chapter 2.....	12
2 Hydrodynamics of a Gas-Driven Gas-Liquid-Solid Spouted Bed with Draft Tube	12
2.1 Background information	12
2.2 Experimental apparatus and methods	17
2.2.1 Experiment apparatus.....	17
2.2.2 Particle properties	18
2.2.3 Measurement methods	20
2.3 General description of gas driven gas-liquid-solid spouted bed.....	23
2.4 Regime transition velocities.....	27
2.4.1 Minimum spouting velocity	27

2.4.2	Full spouting velocity	28
2.4.3	Minimum circulating velocity.....	29
2.5	Effects of operating conditions	30
2.5.1	Draft tube length	30
2.5.2	Nozzle-tube gap	33
2.5.3	Particle density.....	36
2.6	Particle accumulation rate measurement	38
2.7	Summary.....	41
	References	42
Chapter 3	45
3	Hydrodynamics in Gas-Driven Gas-Liquid-Solid Spouted Bed without a Draft Tube	45
3.1	Background information	45
3.2	Experimental apparatus and methods	48
3.2.1	Experimental apparatus.....	48
3.2.2	Particle properties	49
3.2.3	Methods.....	50
3.3	Result and discussion.....	51
3.3.1	Attempt of spouting regime construction	51
3.3.2	Effect of gas flowrate on dead zone length.....	52
3.3.3	Effect of initial static bed height on dead zone length.....	53
3.3.4	Effect of water level on dead zone length.....	54
3.4	Summary	56
	Reference	57
Chapter 4	59
4	Conclusions and Future Work.....	59
4.1	Conclusions.....	59

4.2 Future Work	60
Appendices.....	61
Appendix A. Example of error analysis	61
Appendix B. Rotameter calibration.....	63
Appendix C. Data of experiments	65
Curriculum Vitae	77

List of Tables

Table 2.1 Previous studies for non-conventional spouted bed	14
Table 2.2 Experimental particle properties	19
Table 2.3 Operating conditions of this work	26
Table 2.4 Deviation of calculated and experimental w_p	40
Table 3.1 Properties of particle	50

List of Figures

Figure 1.1 Particle motion in spouted bed configurations. Arrows indicate direction of solids motion.	2
Figure 1.2 Spouted bed flow regimes with increasing gas flow.	3
Figure 1.3 Particle motion in spouted bed with a draft tube. Arrows indicate direction of solids motion.	4
Figure 1.4 Sketch of gas-driven gas-liquid-solid spouted bed with draft tube. Arrows indicate direction of gas motion.	6
Figure 1.5 Regime transition with increasing superficial gas velocity (a) fixed bed; (b) semi spouted bed; (c) full spouted bed; (d) internal circulating fluidized bed.	7
Figure 1.6 Sketch of the proposed gas-driven gas-liquid-solid spouted bed without draft tube. Arrows indicate direction of gas flow.	8
Figure 2.1 Particle moving track in spouted bed	13
Figure 2.2 Four regions in gas-driven gas-liquid-solid spouted bed	16
Figure 2.3 Apparatus of gas-driven gas-liquid-solid spouted bed with draft tube.	18
Figure 2.4 Images of particles used in the experiment (unit of ruler is cm)	19
Figure 2.5 Typical pressure drop in gas-solid spouted bed	21
Figure 2.6 Experimental pressure drop profile in	21
Figure 2.7 Schematic of gas-driven gas-liquid-solid spouted bed with draft tube (Arrows indicate direction of gas motion)	23
Figure 2.8 Regime transition with increasing superficial gas velocity (a) fixed bed; (b) semi spouted bed; (c) full spouted bed; (d) internal circulating fluidized bed	25
Figure 2.9 Particle accumulation rate versus superficial gas velocity	28

Figure 2.10 Particle velocity in the annulus versus superficial gas velocity	29
Figure 2.11 Dense phase retraction versus superficial gas velocity	30
Figure 2.12 Effect of draft tube length on minimum spouting velocity	31
Figure 2.13 Effect of draft tube length on full spouting velocity	32
Figure 2.14 Effect of draft tube length on minimum circulating velocity	33
Figure 2.15 Nozzle-tube gap effect on full spouting velocity	34
Figure 2.16 Nozzle-tube gap effect on minimum circulating velocity	35
Figure 2.17 Particle density effect on minimum spouting velocity	36
Figure 2.18 Particle density effect on full spouting velocity	37
Figure 2.19 Particle density effect on minimum circulating velocity.....	38
Figure 2.20 Comparison of experimental particle accumulation and calculated particle accumulation in basket.....	40
Figure 3.1 Schematic diagram of a spouted bed. Arrows indicate direction of solids motion.	46
Figure 3.2 Flow regime transition with increasing gas flow	47
Figure 3.3 Apparatus of gas-driven gas-liquid-solid spouted bed without draft tube	49
Figure 3.4 Particle motion and dead zone at wall above the nozzle exit level	51
Figure 3.5 Dead zone length variance with gas flowrate (ABS particle)	53
Figure 3.6 Dead zone length variance with initial static bed height (ABS particle)	54
Figure 3.7 Dead zone length variance with water level (a) $H_s=45\text{cm}$, (b) $H_s=30\text{cm}$ (ABS particle)	55

List of Appendices

Appendix A. Example of error analysis	61
Appendix B. Rotameter calibration	63
Appendix C. Data of experiments	65

Nomenclature

Ar	Archimedes number
C_D	Drag coefficient
D_b	Diameter of basket (mm)
D_i	Inner diameter of Column (mm)
D_t	Inner diameter of draft tube (mm)
d_n	Inner diameter of nozzle (mm)
g	Gravitational acceleration (m/s^2)
H_e	Nozzle-tube gap (mm)
H_{de}	Dense phase height in annulus region (mm)
H_{de0}	Initial dense phase height (mm)
H_s	Initial static bed height (mm)
H_w	Water level higher than initial static bed height (mm)
L_d	Draft tube length (mm)
L_n	Non-mobile zone length at column wall (mm)
m_p	Particle mass in basket (g)
Δh	Vertical distance (mm)
Δp	Pressure drop in annulus region (cmH ₂ O)

Δt	Time variation (s)
Q_g	Gas flowrate (l/min)
Re	Reynolds number
u_g	Superficial gas velocity (mm/s)
u_{mfs}	Full spouting velocity (mm/s)
u_{ms}	Minimum spouting velocity (mm/s)
u_p	Particle velocity in annulus (mm/s)
u_t	Terminal velocity (mm/s)
w_p	particle mass accumulation rate (g/s)
w_{pb}	Particle mass accumulation rate in the basket (g/s)
ρ	Density of fluid (kg/m ³)
ρ_p	Density of particle (kg/m ³)
ρ_b	Bulk density of particle (kg/m ³)
ρ_w	Density of water (kg/m ³)
μ_w	Viscosity of water (Pa • s)

Chapter 1

1 General Introduction

1.1 Background

A conventional gas-solid spouted bed contains a vessel filled with coarse particles and fluid injected vertically at the center of the column bottom. The fluid injection results in an upwards movement of particles at the center of the column until they break through the static bed and fall back into the annulus region due to gravity. This is the basic particle flow regime of a spouted bed (Epstein & Grace, 2011). Once the spouted bed flow regime is stable, this system can be divided into four regions, as shown in Figure 1.1, which includes the spouting region, fountain region, annulus region and dead zone. The spouting region is usually at the center of the column above the fluid inlet nozzle where the particles rise quickly with relatively lower concentration and directly influenced by the fluid flow. The region surrounding the spout region is referred as the annulus region, where particles fall downwards slowly at much higher concentrations. The fountain region is located above the bed surface, where particles reach their highest position and then fall back to the annulus region. The previous zones provide the general description of the solids circulation pattern. At the base of the column, there is a region where the particles remain non-mobile, generally referred as the dead zone (Epstein & Grace, 2011).

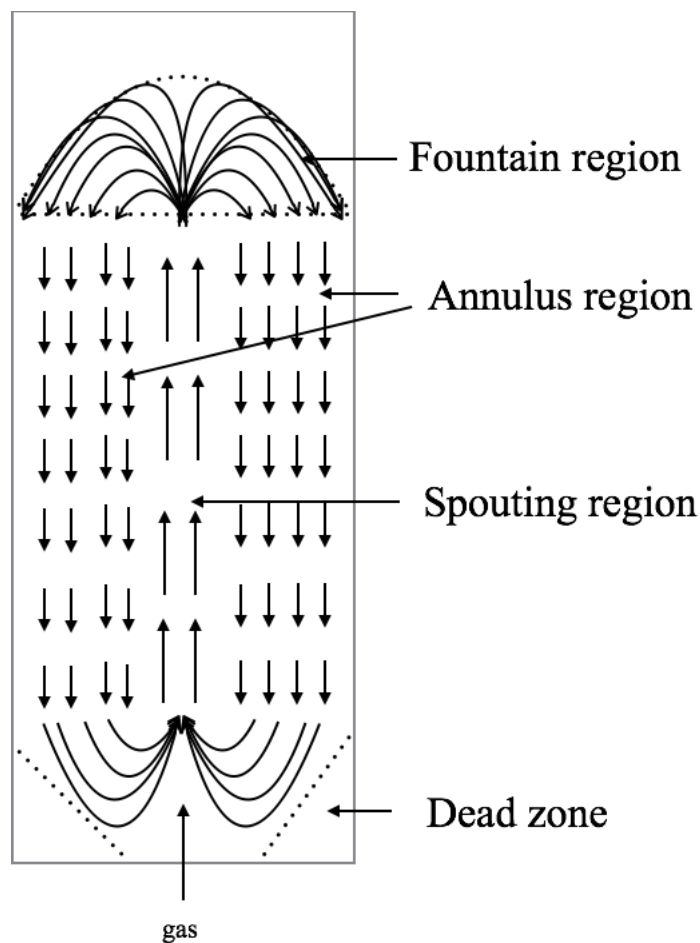
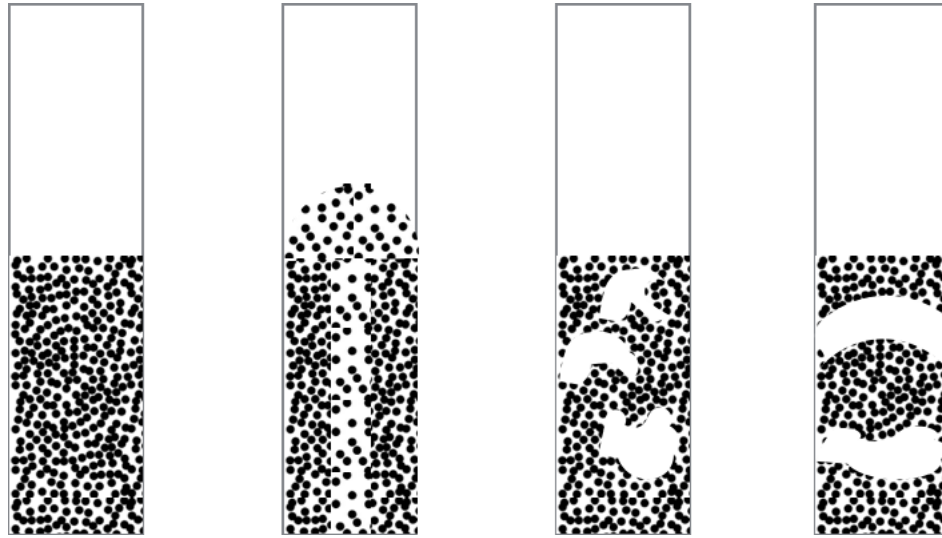


Figure 1.1 Particle motion in spouted bed configurations. Arrows indicate direction of solids motion.

Figure 1.2 illustrates the regime transitions of gas-solid spouted beds when increasing the gas superficial velocity (Epstein & Grace, 2011). The fixed packed bed may however directly change from packed bed into a bubbling bed, as a stable spouted bed may not be developed when the initial static bed height is higher than the maximum spoutable height of this system (Epstein & Grace, 2011). This is because the gas leaks from spouting region to annulus region, breaking the spouting regime when the static bed height is higher than the maximum spoutable height (Mathur & Epstein, 1974). The leaking gas fluidizes the particles in the annulus region and prevents them from falling down. A draft tube can be added in the middle of the column to prevent gas leakage

and eliminate the static bed height limitation. In addition, the draft tube can prevent solids cross flow between spouting region and annulus region (Neto et al., 2008), as illustrated in Figure 1.3.



(a) Static bed (b) Spouted bed (c) Bubbling bed (d) Slugging bed

Figure 1.2 Spouted bed flow regimes with increasing gas flow.

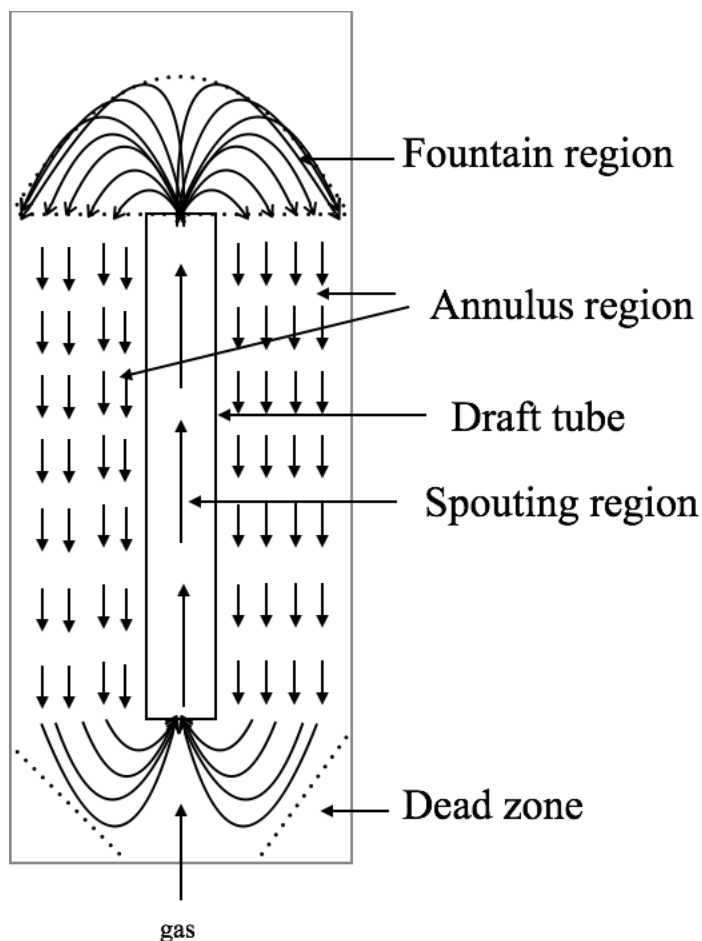


Figure 1.3 Particle motion in spouted bed with a draft tube. Arrows indicate direction of solids motion.

The gas-solid spouted bed was first invented by Mathur and Gisher in the 1950's (Mathur & Gisher, 1955) as an efficient high heat transfer equipment to dry wheat. It then gradually began to see use in many other industry processes, such as gasification (Jarunthammachote & Dutta, 2008), catalytic polymerizations (Olazar et al., 1994), biomass pyrolysis (Amutio et al., 2011) and tablets coating (Kucharski & Kmiec, 1983).

Novel spouted beds were periodically proposed, including a liquid-solid spouted bed (Grbavcic et al., 1992) and a liquid-driven gas-liquid-solid spouted bed (Wang et al. 2003). These systems require liquid net flow to form stable spouting phenomenon. However, research has not been done about the gas-driven gas-liquid-solid spouted bed, which uses only gas flow to form

spouting. Therefore, a new system is proposed that utilizes gas only to form a spouted bed. Gas-liquid-solid spouted bed has a high potential to be used in wastewater treatment processes when the liquid net flowrate through the system is limited, such as the aeration process unit. In this application, the gas-driven system stands out as the energy input required to spout particles can be provided by the aeration gas so that there is no need to recirculate the liquid to form spouting. Therefore, the energy consumption for liquid net flow is saved.

This work therefore proposes a gas-liquid-solid spouted bed driven by gas flow only to form a stable spouted regime and the development of the required measurements methods for regime transition. Figure 1.4 shows a typical sketch of a gas-driven gas-liquid-solid spouted bed with draft tube. Particles are loaded in the cylindrical column. A nozzle at the center of the column base injects gas vertically into the system. There is no liquid net flow as the gas is the only driven factor in this system.

A gas-driven gas-liquid-solid spouted bed can be described based on the same four regions as the gas-solid spouted bed. However, the resulting flow regimes when increasing the gas flow rate, as shown in Figure 1.5, differ from the gas-solid configuration. Particle circulation is first developed near the outside of the draft tube and then expands to the entire annulus region. The flow regime finally changes to internal circulating fluidized bed at higher superficial gas velocities. The superficial gas velocity which spouts and circulates the particles near the outside of the draft tube is called the minimum spouting velocity (u_{ms}), while the velocity which spouts the whole system is called the full spouting velocity (u_{mfs}). For these flow regimes, the particles in the annulus region move downward and come in contact with each other. The particles thus form a dense phase in the annulus and a dilute phase in fountain, as shown in Figure 1.5 (b) and (c). Above a certain superficial gas velocity, referred as the minimum circulating velocity, the dense phase is eliminated. The spouted bed is then operating as an internal circulating fluidized bed where all the particles are fluidized (Gokon et al., 2008), as shown in Figure 1.5 (d).

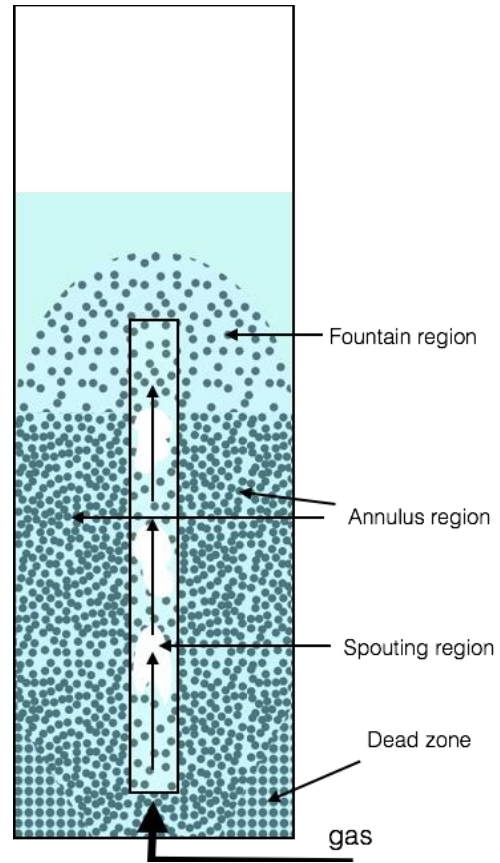


Figure 1.4 Sketch of gas-driven gas-liquid-solid spouted bed with draft tube. Arrows indicate direction of gas motion.

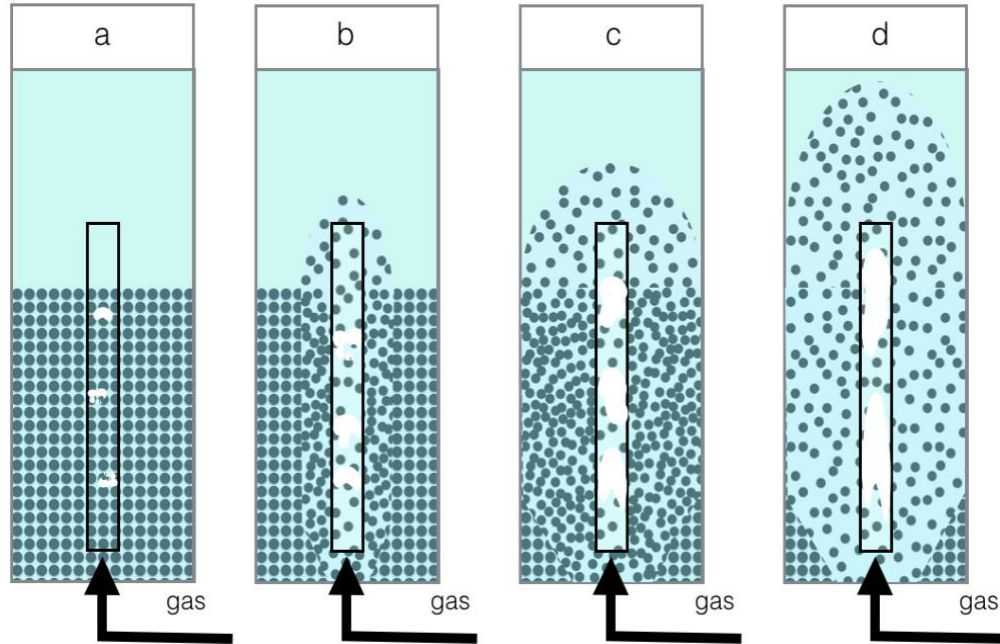


Figure 1.5 Regime transition with increasing superficial gas velocity (a) fixed bed; (b) semi spouted bed; (c) full spouted bed; (d) internal circulating fluidized bed.

A gas-driven gas-liquid-solid spouted bed without a draft tube is also studied in this work, as shown in Figure 1.6. The nozzle at the center introduces a vertical gas jet in this system to form a spout. Again, there is no liquid net flow in this system. Similar to the gas driven system with a draft tube, it has four regions to describe the particle flow. The dead zone length at wall (L_n) is studied to better understand the design of future conical bottoms to avoid creation of a dead zone and to maximize the useful volume of the contactor (Jose et al., 1996).

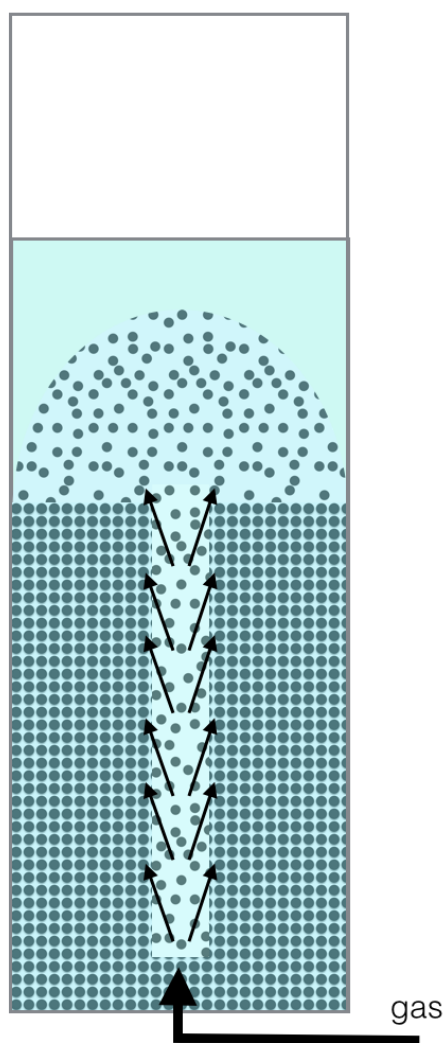


Figure 1.6 Sketch of the proposed gas-driven gas-liquid-solid spouted bed without draft tube. Arrows indicate direction of gas flow.

1.2 Thesis objectives

The main objective of this thesis is to develop and characterize a novel gas-driven gas-liquid-solid spouted bed and to gain a basic understanding of its overall hydrodynamics. The specific objectives of this work can be further described as:

1. Design and construct a gas-driven gas-liquid-solid spouted bed.
2. Develop suitable measurement methods for relevant hydrodynamic characteristics in the gas-driven gas-liquid-solid spouted bed with draft tube, including minimum spouting velocity (u_{ms}), full spouting velocity (u_{mfs}) and minimum circulating velocity (u_{ci}).
3. Investigate the impacts of draft tube length (L_d), nozzle-tube gap (H_e) and particle density (ρ_p) on the minimum spouting velocity (u_{ms}), full spouting velocity (u_{mfs}) and minimum circulating velocity (u_{ci}).
4. Investigate the impact of static bed height (H_s), water level (H_w), and gas flowrate (Q_g) on the dead zone length at wall (L_n) in the gas-driven gas-liquid-solid spouted bed without a draft tube.

1.3 Thesis structure

This thesis contains four chapters:

Chapter 1 provides a general introduction, the thesis objectives, and the thesis structure.

Chapter 2 investigates the gas-driven gas-liquid-solid spouted bed with a draft tube. The effects of draft tube length, nozzle-tube gap and particle density on regime transition velocities including minimum spouting velocity, full spouting velocity, minimum circulating velocity. Comparison of two methods to measure particle accumulation rate is also provided.

Chapter 3 investigates the gas-driven gas-liquid-solid spouted bed without a draft tube. The effects of water level, initial static bed height and gas flowrate on the dead zone length at wall are studied.

Chapter 4 provides the conclusions of this research and recommendations for future work.

Reference

- Amutio, M., Lopez, G., Artetxe, M., Elordi, G., Olazar, M., & Bilbao, J. (2011). Influence of temperature on biomass pyrolysis in a conical spouted bed reactor. *Resources, Conservation and Recycling*. **59**, 23-31
- Epstein, N., & Grace, J.R. (2011). *Introduction*. Chapter 1 of *Spouted and Spout-Fluid Beds* edited by Epstein, N. & Grace, J. Cambridge, UK
- Gokon, N., Takahashi, S., Yamamoto, H., & Kodama, T. (2008). Thermochemical two-step water-splitting reactor with internally circulating fluidized bed for thermal reduction of ferrite particles. *International Journal of Hydrogen Energy*. **33**, 2189-2199
- Grbavcic, Z., Vukovic, D., Jovanovic, S., Garic, R., Hadzismajlovic, D., Littman, H., & Morgan, M. (1992). Fluid flow regime and solids circulation rate in a liquid phase spout-fluid bed with draft tube. *The Canadian Journal of Chemical Engineering*. **70**, 895-904
- Jarunghammachote, S. & Dutta, A. (2008). Equilibrium modeling of gasification: Gibbs free energy minimization approach and its application to spouted bed and spout-fluid bed gasifiers. *Energy Conversion and Management*. **49**, 1345-1356
- Jose, M., Olazar, M., Llamosas, R., Izquierdo, M., & Bilbao, J. (1996). Study of dead zone and spout diameter in shallow spouted beds of cylindrical geometry. *The Chemical Engineering Journal*. **64**, 353-359
- Kucharski, J., & Kmiec, A. (1983). Hydrodynamics, heat and mass transfer during coating of tablets in a spouted bed. *The Canadian Journal of Chemical Engineering*. **61**, 435-439.
- Mathur, K.B., & Gisher, P. (1955). A study of the application of the spouted bed technique to wheat drying. *Journal of Applied Chemistry*. **5**, 624-636
- Mathur, K. & Epstein, N. (1974). *Spouted bed*, Academic Press, New York. USA

Neto, V., Duarte, C., Murata, V., & Barrozo, M. (2008). Effect of a draft tube on a fluid dynamics of a spouted bed: experimental and CFD studies. *Drying Technology*. **26**, 299-307

Olazar, M., Jose, M., Zabala, G. & Bilbao, J. (1994). New reactor in jet spouted bed regime for catalytic polymerizations. *Chemical Engineering Science*. **49**, 4579-4588

Wang, J., Wang, T., Liu, L., & Chen, H. (2003). Hydrodynamics behavior of a three-phase spouted bed with very large particles. *The Canadian Journal of Chemical Engineering*. **81**, 861-866

Chapter 2

2 Hydrodynamics of a Gas-Driven Gas-Liquid-Solid Spouted Bed with Draft Tube

2.1 Background information

Gas-solid spouted beds were invented in 1955 and initially used as a fluidized bed configuration designed to dry wheat in Canada (Mathur & Gisher, 1955). The configuration was gradually used in other chemical engineering processes, including solids blending, gas cleaning and thermal cracking (Markowski & Kaminski, 1983). A conventional gas-solid spouted bed generally consists of a vertical cylindrical vessel filled with particles where gas is injected from a nozzle at the bottom of the column. The injected gas provides the necessary drag force on the particles (Epstein & Grace, 2011) to result in an upward flow of the particles at the center of the column until break through the static bed and fall back into the annulus region due to gravity.

The typical solids circulation pattern for a gas-solid spouted bed, shown in Figure 2.1 (Epstein & Grace, 2011), consists of four regions including the spouting region, annulus region, fountain region and dead zone. Particles move upward with high velocity and low concentration in the spouting region, which is driven by the drag force and buoyancy force of the fluid flow (Epstein & Grace, 2011). The particles then reach the fountain region where they move to the surrounding and transition from a rising to a falling state. Next, the particles travel downward with low velocity and high concentration due to gravity. Finally, the falling particles move from the annulus region to the spouting region, repeating the same cycle. This concludes the circulating process of particles in spouted bed. At the bottom of a flat bottom spouted bed, particles close to the bottom walls of the bed cannot be removed by both gravity and fluid flow, forming a dead zone. The spouting regime can be broken by increasing gas velocity and form a bubbling and slugging regime (Epstein & Grace, 2011).

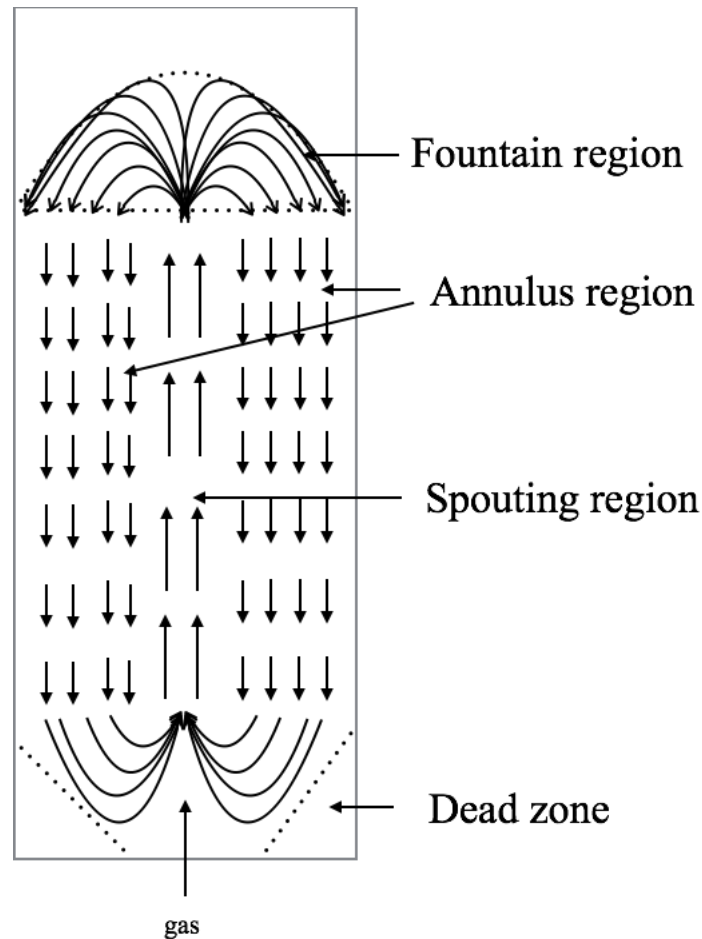


**Figure 2.1 Particle moving track in spouted bed
(Arrows indicate direction of solids motion)**

To expand the application of spouted beds, non-conventional spouted bed configurations were proposed to address the needs of specific processes including liquid-solid spouted beds (Grbavcic et al., 1992) and liquid-driven gas-liquid-solid spouted beds (Wang et al. 2003). Table 2.1 shows the prior work of some researchers about the liquid-solid and liquid-driven gas-liquid-solid spouted bed (Grbavcic et al. 1992; Littman et al., 1974; Anabtawi et al. 2003; Vukovic et al. 1974; Wang et al., 2003; Erbil, 2005), which focus on liquid-solid and liquid-driven gas-liquid-solid systems.

Table 2.1 Previous studies for non-conventional spouted bed

Type of bed	Researcher	Fluid	Particle Property	Column and Nozzle Diameter	Experiment Objective
Liquid-Solid	Grbavcic et al. 1992	Water injected from the nozzle and uniformly distributed in the annulus region	Glass bead ($\rho_p=2641\text{kg/m}^3$) with diameter 1.20mm; Glass bead ($\rho_p=2507\text{kg/m}^3$) with diameter 1.94mm; Glass bead ($\rho_p=2509\text{kg/m}^3$) with diameter 2.98mm;	Semi cylindrical column:196mm ID Nozzle: 33mm	Fluid flow regime and solids circulation rate
Gas-Liquid-Solid	Littman et al. 1974	Gas injected from nozzle. Water injected from nozzle and uniformly distributed in the annulus region	Glass bead ($\rho_p=2500\text{kg/m}^3$) with diameter 3.09mm	Cylindrical column: 62.6mm ID Rectangular Nozzle: 4.3mm*7.3mm*9.3mm	Hydrodynamics in three phases spouted bed
Gas-Liquid-Solid	Anabtawi et al. 2003	Spouting air injected from the central nozzle. Air and water uniformly distributed in the annulus	Glass bead ($\rho_p=2600\text{kg/m}^3$) with diameter 1.75mm	Cylindrical column: 74mm, 114mm, 144mm ID Nozzle: 10mm ID	Oxygen absorption
Gas-Liquid-Solid	Vukovic et al. 1974	Air injected from the central nozzle and water uniformly distributed from the head located at the central top of the column	Hollow polyethylene sphere ($\rho_p=320\text{kg/m}^3$) with diameter 10mm	Column: 194mm ID Nozzle: 30mm ID	Hydrodynamics in the three phases spouted bed

Gas-Liquid-Solid	Wang et al. 2003	Water injected from the nozzle and air introduced from a ring type distributor	Glass bead ($\rho_p=2200\text{kg/m}^3$) with diameter 10.5mm, 12.0mm, 16.0mm	Column: 230mm ID Nozzle: 16mm ID	Influence of superficial gas velocity, liquid circulation velocity, minimum liquid spouting velocity, pressure drop
Gas-Liquid-Solid	Erbil 2005	Pulse injected into the spout region. Water pulse introduced into the annulus region. Additionally, air uniformly introduced into annulus region.	Glass bead ($\rho_p=2533\text{kg/m}^3$) with diameter 3mm	Semi-cylindrical column: 80mm ID Nozzle: 10mm ID	Effect of annulus leakage on particle circulation

The previous studies on non-conventional spouted beds included liquid-driven or gas-liquid driven systems. Liquid net flow is necessary to spout the particles. However, research has not been done about the gas-driven gas-liquid-solid spouted bed, which uses only gas flow to form spouting. Therefore, a new system is proposed that utilizes gas only to form a spouted bed. Gas-liquid-solid spouted bed has a high potential to be used in wastewater treatment processes when the liquid net flowrate through the system is limited, such as the aeration process unit. In this application, the gas-driven system stands out as the energy input required to spout particles can be provided by the aeration gas so that there is no need to recirculate the liquid to form spouting. Therefore, the energy consumption for liquid net flow is saved.

To maintain good stability in a proposed gas-driven gas-liquid-solid spouted bed, gas is injected from a central nozzle at the bottom of a cylindrical column filled with particles and stagnant

water. The gas injection results in an upward movement of the particles at the center of the column until they break through the static bed and fall back into the annulus region due to gravity. The spouting for a gas-driven gas-liquid-solid spouted bed share similarity with the gas-solid system including the four regions phenomenon and particle circulation behavior. Additionally, a draft tube may be added into this system to avoid gas leakage and particle crossing from the spouting region to the annulus region as shown in Figure 2.2. The goal of this work is to form the spouting phenomenon by gas flow only and study hydrodynamics in this system including regimes and regime transition velocities.

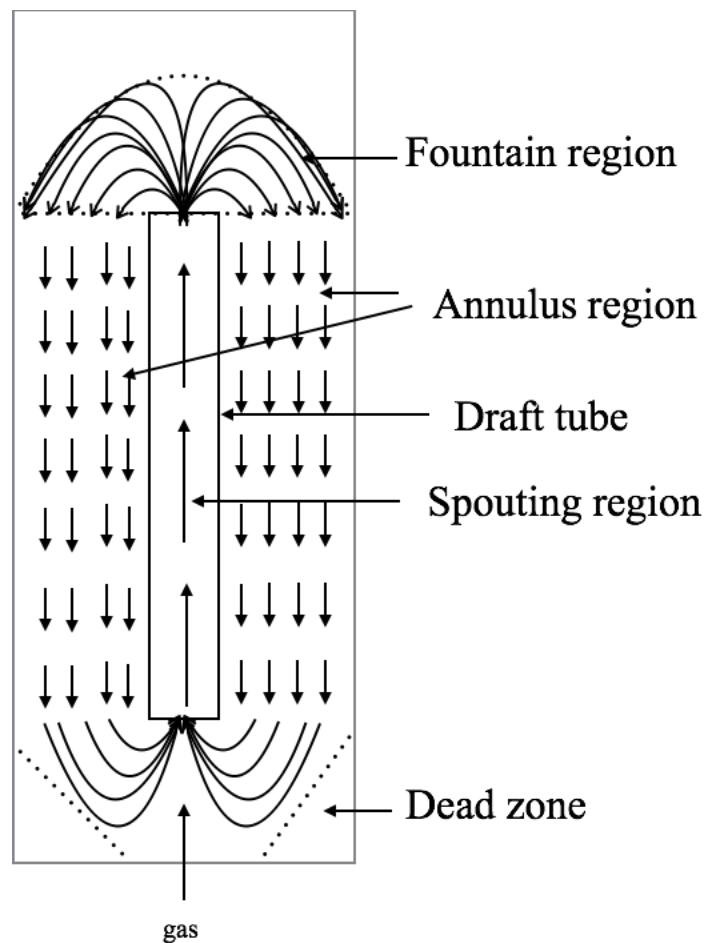


Figure 2.2 Four regions in gas-driven gas-liquid-solid spouted bed (Arrows indicate particle motion)

2.2 Experimental apparatus and methods

2.2.1 Experiment apparatus

Figure 2.3 presents a schematic of the gas-driven gas-liquid-solid spouted bed used in this work. Water and air are used as the liquid and gas phases, respectively. The vertical column is made of transparent plexiglass with 152 mm (6 inch) inner diameter (D_i) and 6 mm thickness is open to the atmosphere. A draft tube with 52 mm inner diameter (D_t) and 4 mm thickness sits at the center of the column, while the length is varied to investigate the effect of the draft tube length (L_d) on the hydrodynamics in this system. Three pressure ports located at the column wall are used to measure the pressure drop in the annulus region. The gas injection nozzle at the center and bottom of the column has an inner diameter (d_n) of 4.5 mm and 1 mm thickness. The water level is maintained at 600mm higher than the initial static bed height. A basket with 36 mm inner diameter, 4 mm thickness and 130 mm height is placed in the annulus region, with its open-top slightly above the initial static bed and allowing the measurement of the particle accumulation rate. The nozzle-tube gap (H_e) and the draft tube length (L_d) are varied to find their effects on the studied hydrodynamics. The superficial gas velocity reported in this work is the volumetric gas flowrate divided by the cross-sectional area of the larger column (i.e., 152 mm diameter).

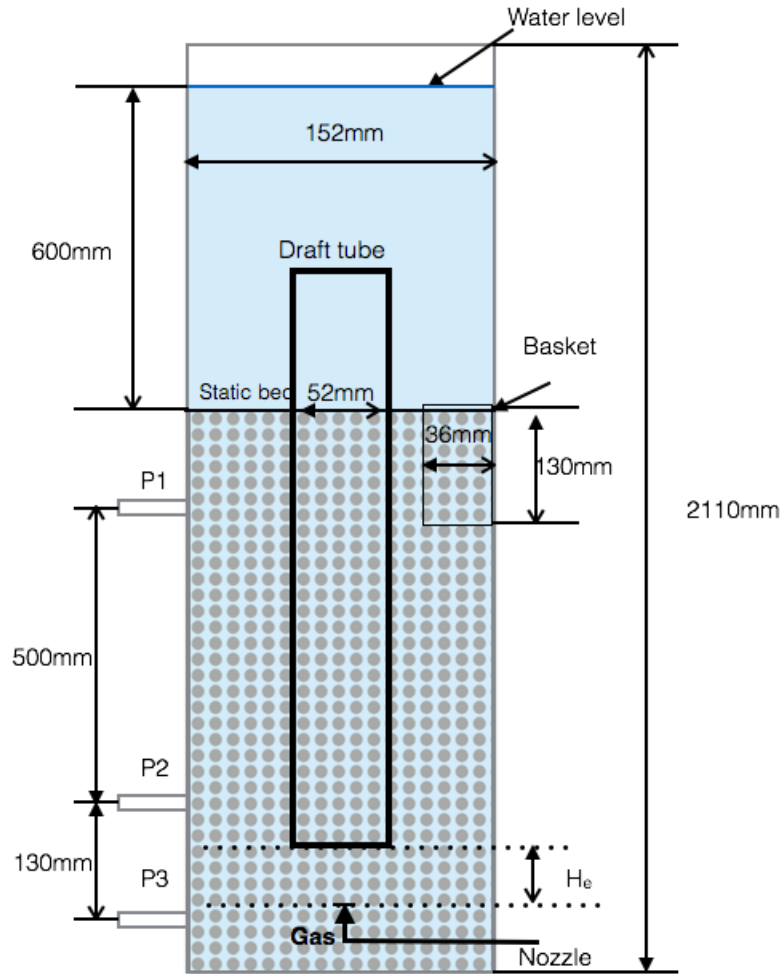


Figure 2.3 Apparatus of gas-driven gas-liquid-solid spouted bed with draft tube

2.2.2 Particle properties

Three types of particles were investigated in this study including Acrylonitrile Butadiene Styrene (*ABS*) particles and two types of plastic particles. Figure 2.4 provides a visual comparison of the particles and Table 2.2 provides the particle properties. The *ABS* particle size distribution is narrow.

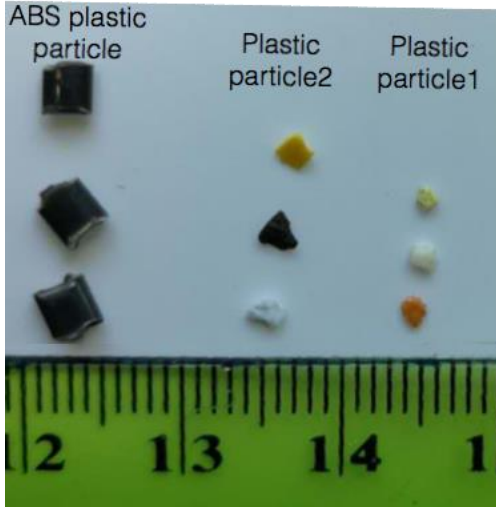


Figure 2.4 Images of particles used in the experiment (unit of ruler is cm)

Table 2.2 Experimental particle properties

Particle Type	Particle Density (kg/m^3)	Bulk Density (kg/m^3)	Particle size (mm)	Volume Equivalent Diameter (mm)	Archimedes Number (-)	Terminal Velocity in Liquid (m/s)
ABS particle	1044	644	2.5	2.5	6738	0.036
Plastic particle 1	1348	803	0.6-0.8	0.7	1170	0.011
Plastic particle 2	1485	819	1.3-1.7	1.5	15711	0.062

Archimedes number and terminal velocities were calculated using the following equations (Khan & Richardson, 1988):

$$Ar = \frac{3}{4} C_{Dt} Re_t^2 = d_p^3 \rho (\rho_s - \rho) g / \mu^2 \quad (2.1)$$

$$Re_t = (2.33 Ar^{0.018} - 1.53 Ar^{-0.016})^{13.3} \quad (2.2)$$

$$u_t = \frac{\mu Re_t}{d_p \rho_p} \quad (2.3)$$

2.2.3 Measurement methods

In a gas-solid spouted bed, the minimum spouting velocity (u_{ms}) is defined as the gas velocity corresponding to the point at which stable external spouting collapses with decreasing gas flowrate (Epstein & Grace, 2011). It is generally determined by measuring the pressure drop (Δp) across the bed height as a function of superficial gas velocity in a traditional spouted bed. For a typical measurement, the pressure drop increases from 0 until reaching a peak value, and then decreases to a constant value. The minimum spouting velocity is the superficial gas velocity when the pressure drop becomes constant, as shown in Figure 2.5 (Mathur & Epstein, 1974).

The pressure drop method, however, cannot be used to identify the minimum spouting velocity for the gas-drive gas-liquid-solid spouted bed. For the gas-driven system, the pressure drop decreases continuously when increasing the superficial gas velocity, as shown in Figure 2.6. This measurement difference is mainly because the particle density used in this work is very close to water, the continuous phase in this system. The pressure drop variance caused by particles cannot be readily distinguished by the pressure drop method, as shown in Equation 2.4. Furthermore, the water motion also affects the pressure drop across the bed, making it more difficult to use pressure drop method to find minimum spouting velocity.

$$\Delta p = (\rho_p + \rho_w)g \Delta h \quad (2.4)$$

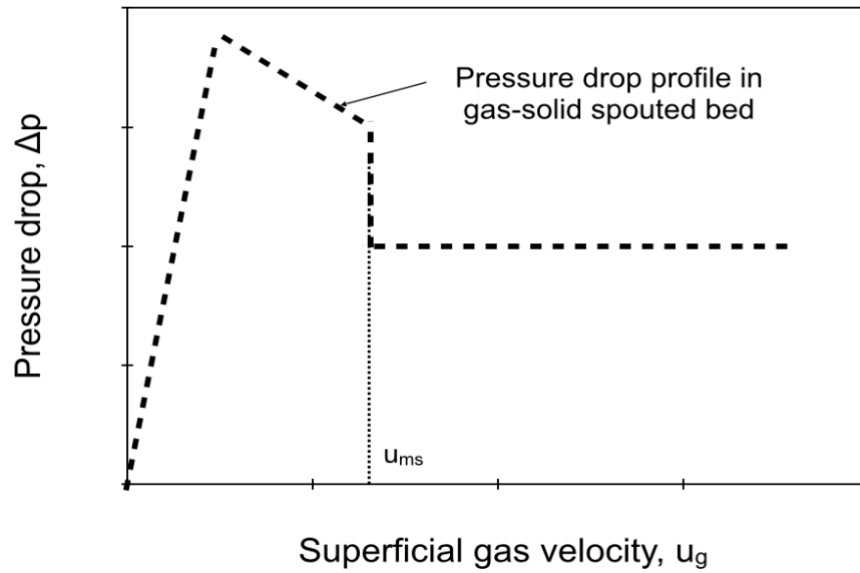


Figure 2.5 Typical pressure drop in gas-solid spouted bed

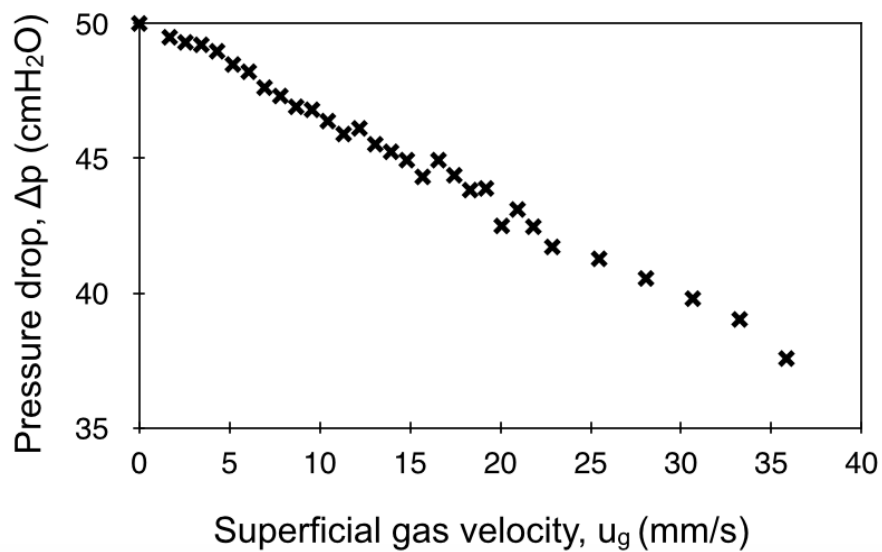


Figure 2.6 Experimental pressure drop profile in gas-driven gas-liquid-solid spouted bed

The minimum spouting velocity was thus determined by measuring the particle accumulation rate (w_p) in the gas-driven gas-liquid-solid spouted bed. The particle accumulation rate was measured using a basket. The basket is a plexiglass tube with 13 mm length, 36 mm inner

diameter and 4 mm thickness. It has a lid on the top and mesh at bottom. In the measurement, the basket was placed in the annulus region and the top of the basket is maintained just above as the static bed height. Once the system forms a stable solid circulating pattern, the lid of basket is opened, allowing the particles to enter the basket. The basket is then covered again and taken out, allowing the particles within it to be dried. Finally, the particles are weighed by a balance and the particle accumulation rate is calculated by Equation 2.5.

$$W_p = \frac{m_p}{\Delta t} \quad (2.5)$$

where $\Delta t = 50s$

The full spouting velocity is determined by measuring the particle velocity in the annulus via video analysis. The particles in annulus move downward as packed bed. A 20 second video is taken between 20 cm to 40 cm from bottom level range of the column. Three particles are selected randomly to estimate the particle velocity, calculated based on the distance travelled (Δh) over a selected time interval, as shown in Equation 2.6. This process is finished by a video processing software Shotcut. In this measurement, the wall effect is neglected.

$$u_p = \frac{\Delta h}{\Delta t} \quad (2.6)$$

where $\Delta t = 20s$.

The minimum circulating velocity is determined based on the dense phase retraction (H_{de}/H_{de0}) in the annulus region. Dense phase height in the annulus can be directly obtained through visual observation. The dense phase retraction is calculated by the dense phase height (H_{de}) over the initial dense phase height (H_{de0}). The observation method is feasible because this is a qualitative comparison.

2.3 General description of gas driven gas-liquid-solid spouted bed

Figure 2.7 illustrates the studied gas-driven gas-liquid-solid spouted bed with a draft tube. There is a nozzle at the central bottom of the column for gas inlet into this system. There is no net flow of liquid in and out of the spouted bed and the gas is the only driven factor in this system. Particles are loaded in the annulus region of the cylindrical column. The gas injection forms bubbles and results in an upward movement of particles in the draft tube located at the center of the column until the particles break through the static bed. The particles then fall downward as packed bed in the surrounding region due to gravity and the particles entrain into the draft tube at the bottom. The solid circulating motion is similar to gas-solid spouted beds.

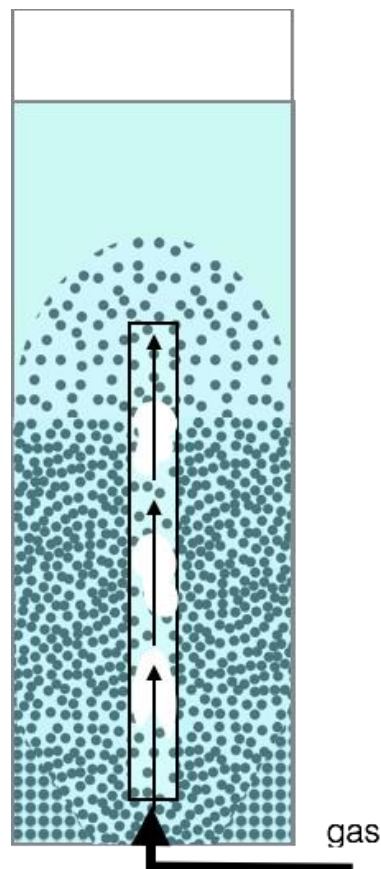


Figure 2.7 Schematic of gas-driven gas-liquid-solid spouted bed with draft tube
(Arrows indicate direction of gas motion)

The gas-driven gas-liquid-solid spouted bed can be divided into four regions, including spouting region, annulus region, fountain region and dead zone, similar to gas-solid spouted beds. It has four flow regimes including fixed bed, semi spouted bed, full spouted bed and internal circulating fluidized bed. When gas velocity is low, gas is injected into the column at a flow rate that is not high enough to spout the particles. Particles remain stationary, resulting in a fixed bed regime, as shown in Figure 2.8 (a). As gas flow is increased, more bubbles with higher rising velocities flow through the draft tube, and the particles begin circulating between the spouting region and the partial annulus, transitioning into a semi spouted bed, as illustrated in Figure 2.8 (b). As the gas velocity further increases, more particles in the spouting region are spouted upward and more particles in the annulus region begin moving downwards to compensate. The particles close to column wall are fully in motion which is referred as the full spouted bed and is illustrated in Figure 2.8 (c). Finally, further increasing the gas velocity spouts the particles higher and forms a much larger fountain region. The particles in the annulus region decrease to a point where the dense phase height cannot be observed. The particles in annulus region change from moving downward as packed bed to free falling. thus becoming an internal circulating fluidized bed (Gokon et al, 2008) as shown in Figure 2.8 (d).

The superficial gas velocity which can spout the particles and result in partial solids circulation in the annulus is called minimum spouting velocity (u_{ms}). Gas flow breaks the loose-packed bed in the draft tube. The particles in the spouting region move upwards with high velocity and low concentration. The particles in the annulus close to the draft tube begin moving downward with high concentration and low velocity. Under this gas velocity, the regime changes from the fixed bed to the semi spouted bed, as shown in Figure 2.8 (a) to Figure 2.8 (b). The superficial velocity which can spout the whole system is called full spouting velocity (u_{mfs}). More particles in the annulus region are required to compensate for the spouting region as the particles in the spouting

region move upwards with higher velocity. Therefore, the particles close to the wall begin moving. Under this gas velocity, the regime changes from semi spouted bed to full spouted bed, as shown in Figure 2.8 (b) to Figure 2.8 (c). The superficial gas velocity which can change the particles in the annulus moving downward as packed bed to free falling is called minimum circulating velocity (u_{ci}). Less particles exist in the annulus region as it changes to the dilute phase because the particles in the spouting region move with much higher velocity as well as spouting much higher and forming a bigger fountain, resulting in more particles located in the upper area of the spouted bed. Under this gas velocity, the regime changes from full spouted bed to internal circulating fluidized bed as displayed in Figure 2.8 (c) to Figure 2.8 (d).

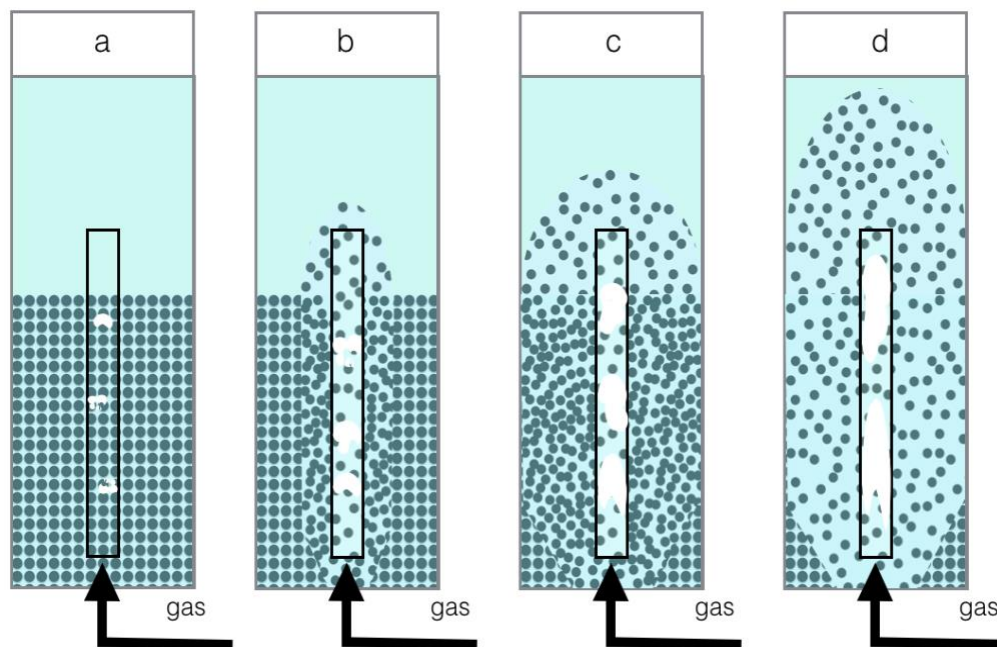


Figure 2.8 Regime transition with increasing superficial gas velocity (a) fixed bed; (b) semi spouted bed; (c) full spouted bed; (d) internal circulating fluidized bed

Three velocities are studied in this project including minimum spouting velocity (u_{ms}), full spouting velocity (u_{mfs}) and minimum circulating velocity (u_{ci}). The flow regime transitions for gas-

driven gas-liquid-solid spouted bed provide important hydrodynamic characteristics for this configuration. In the previous research of spouted bed, it has been found that the particle properties and the bed geometry of structures affect the hydrodynamics in spouted bed, including draft tube length (Grbavicic et al., 1992), nozzle-tube gap (Zhao et al., 2006) and particle density (Mathur & Gisher, 1955). The density difference between liquid and solid can affect the hydrodynamics in this system. Therefore, this project used three kinds of particles with different densities to find the density effect on the regime transition process. ABS particle with different draft tube lengths, nozzle-tube gaps were used to find the effects of geometry factors on the regime transition process. The operating conditions used in this study are summarized in Table 2.3.

Table 2.3 Operating conditions of this work

ABS particles					Plastic particles 1 and 2
Draft tube length, L_d (mm)	300	600		900	900
Initial static bed height, H_s (mm)	300	600		800 900	800
Nozzle-tube gap, H_e (mm)	0	0	20	40	0
Superficial gas velocity, u_g (mm/s)	0-10				0-24

2.4 Regime transition velocities

2.4.1 Minimum spouting velocity

The minimum spouting velocity is the regime transition velocity from fixed bed to semi spouted bed. It is measured by the basket method. The particle accumulation rate can be measured by the collection of particles in the basket located adjacent to the draft tube and the top of the basket is slightly above the top of the initial static bed.

With increasing superficial gas velocity, the particle accumulation rate (w_p) increases, as shown in Figure 2.9. A sharp increase is observed because particle circulation starts when the gas velocity is higher than the minimum spouting velocity. The particle accumulation rate above the minimum spouting velocity (u_{ms}) increases proportionally with superficial gas velocity. This is due to the higher superficial gas velocity spouting more particles in the draft tube as drag force is higher and causing a higher solid circulation rate. There will be a cross point M on the horizontal line and the regression line of this series of measurements. Point M is defined as the minimum spouting velocity. The particle accumulation rate at lower superficial gas velocity is not zero due to the existing particle density distribution. Some particles with lower density can be spouted up at very low superficial gas velocity. This can be neglected as this represents a minor portion of the particles.

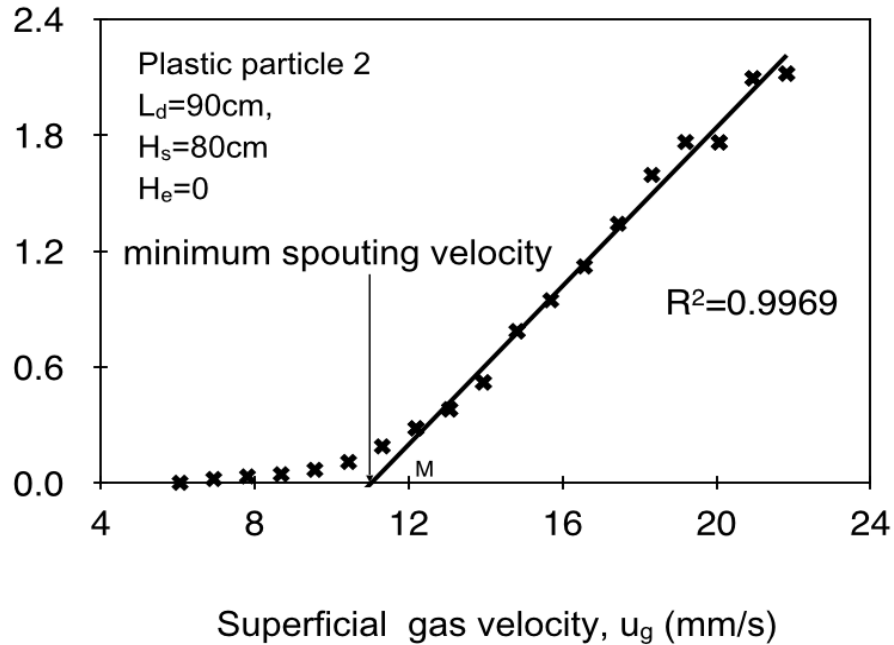


Figure 2.9 Particle accumulation rate versus superficial gas velocity

2.4.2 Full spouting velocity

The full spouting velocity (u_{mfs}) is defined as the superficial velocity when the regime changes from semi spouted bed to full spouted bed. It is determined based on the particle downwards velocity in the annulus at wall (u_p).

With increasing gas velocity, so increases the particle velocity in the annulus, as shown in Figure 2.10. There is a sharp increase because the particles close to the column wall begin moving when the superficial gas velocity is higher than full spouting velocity. At this point, all particles begin moving, except those in the dead zone. The particle velocity in the annulus increases proportionally with superficial gas velocity in the full spouting regime. This is also due to the higher gas velocities spouting more particles in the spouting region. Particles in the annulus region need to compensate for the void created by the higher gas velocity spouting more particles. Therefore, the particle downwards velocity in the annulus region becomes higher. In this process, the impact

of liquid motion is neglected because the particles move downwards as packed bed. There is a cross point N of the horizontal line and the regression line, which is defined as the full spouting velocity.

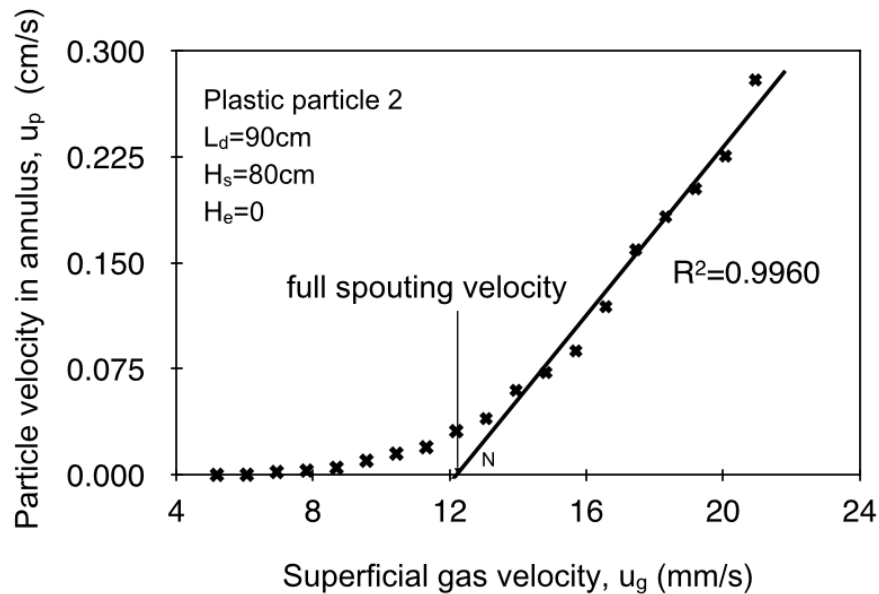


Figure 2.10 Particle velocity in the annulus versus superficial gas velocity

2.4.3 Minimum circulating velocity

The minimum circulating velocity (u_{ci}) is defined as the superficial velocity when the regime changes from full spouted bed to internal circulating fluidized bed. It is determined based on the dense phase retraction method.

With increasing superficial gas velocity, the dense phase retraction is faster, as shown in Figure 2.11. There is a sudden change of dense phase height to zero. This is because the particles in the annulus region to flow to the draft tube is faster than the particle in the fountain to flow to the annulus. Therefore, the dense phase height can no longer be visually determined. The system thus changes to an internal circulating regime. The superficial gas velocity corresponding to this point is defined as the minimum circulating velocity. The dense phase retraction decreases with

increasing the superficial gas velocity. This is because the higher gas velocity forms a bigger fountain region. More particles located in the fountain results in fewer particles in the annulus dense phase region.

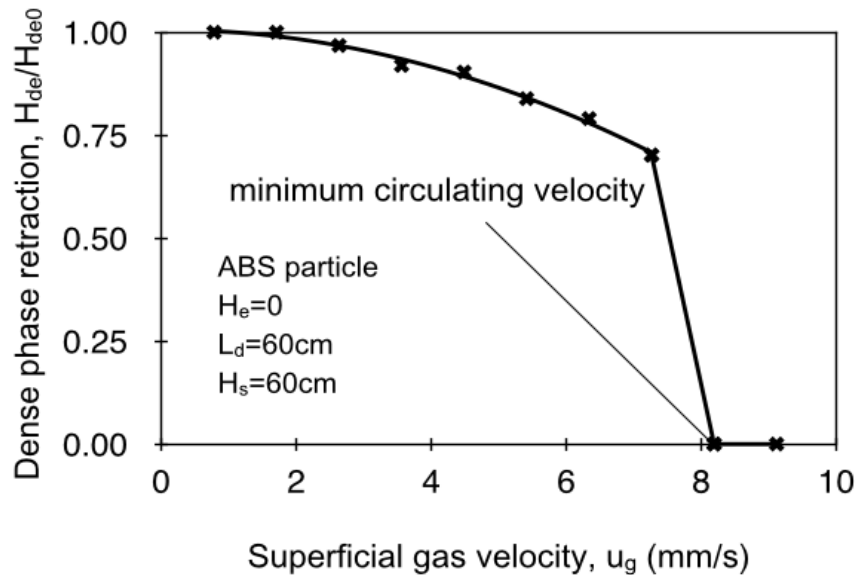


Figure 2.11 Dense phase retraction versus superficial gas velocity

2.5 Effects of operating conditions

2.5.1 Draft tube length

The minimum spouting velocity increases with increasing draft tube length, as shown in Figure 2.12. This phenomenon may be due to the increased solids in the longer draft tube, requiring higher superficial gas velocities to spout. The more particles thus require more fluid flow to break the loose-packed bed. This result agrees with the previous observations in a gas-solid spouted bed (Mathur & Gisher, 1955). In addition, the slopes of these three lines are approximately equal, indicating that the comparable particle accumulation rate increases as a function of superficial gas velocity once the spouting condition is formed. This is because the same increasing of superficial

gas velocity can provide the same increasing of drag force to spout the same weight of particles. The same partial of these particles finally accumulate in the basket. The particle accumulation increasing have the same rate in different groups.

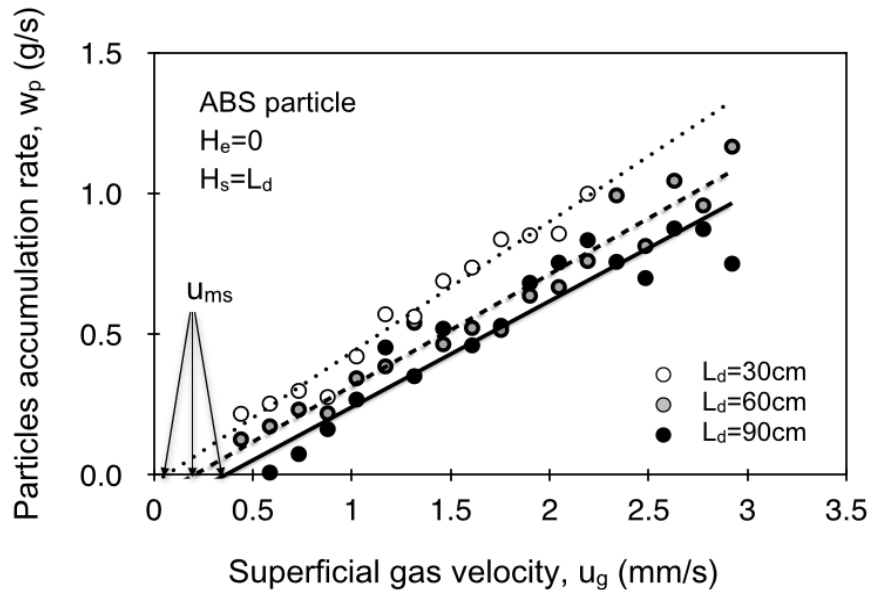


Figure 2.12 Effect of draft tube length on minimum spouting velocity

The full spouting velocity increases with increasing draft tube length, as shown in Figure 2.13. This is because the increasing amount of solid in longer draft tube requires higher superficial gas velocity to break through the loose-packed bed, as explained in Figure 2.12. In addition, a longer draft tube has more particles in the annulus region adjacent to the draft tube. Therefore, the circulation development become slower from center to surrounding and the particles close to the wall require higher superficial gas velocity to move. In addition, the slopes of these two lines are approximately the same, implying that the particle velocity in the annulus region increases proportional with the superficial gas velocity once the system is full spouted. This may be because

the same increasing of superficial gas velocity can spout the same weight of particles, as explained in Figure 2.12. The equivalent weight of particles are required to compensate the spouting region from the annulus region, resulting in the same increased particle moving velocity in the annulus region.

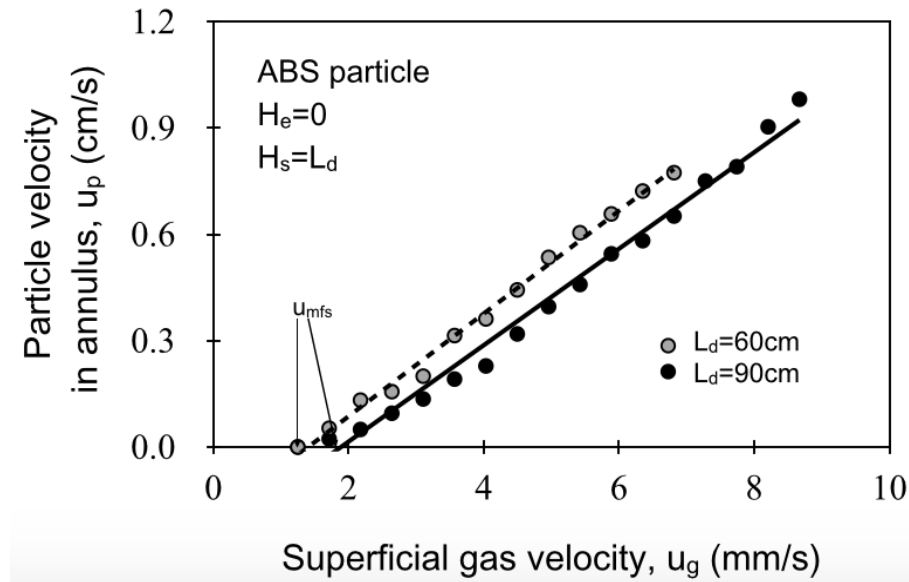


Figure 2.13 Effect of draft tube length on full spouting velocity

The minimum circulating velocity increases with increasing draft tube length, as shown in Figure 2.14. Although the retraction for tube 90cm does not change to zero, it is evident that it has a higher minimum circulating velocity, as illustrated in Figure 2.14. This result was expected as both the minimum spouting velocity and full spouting velocity for a longer draft tube were higher, as explained in Figure 2.12 and Figure 2.13. In addition, increased solids in the annulus region with longer draft tube has a higher dense phase to retract, requiring a higher superficial gas velocity. Therefore, a longer draft tube group requires a higher gas velocity to form a internal circulating bed

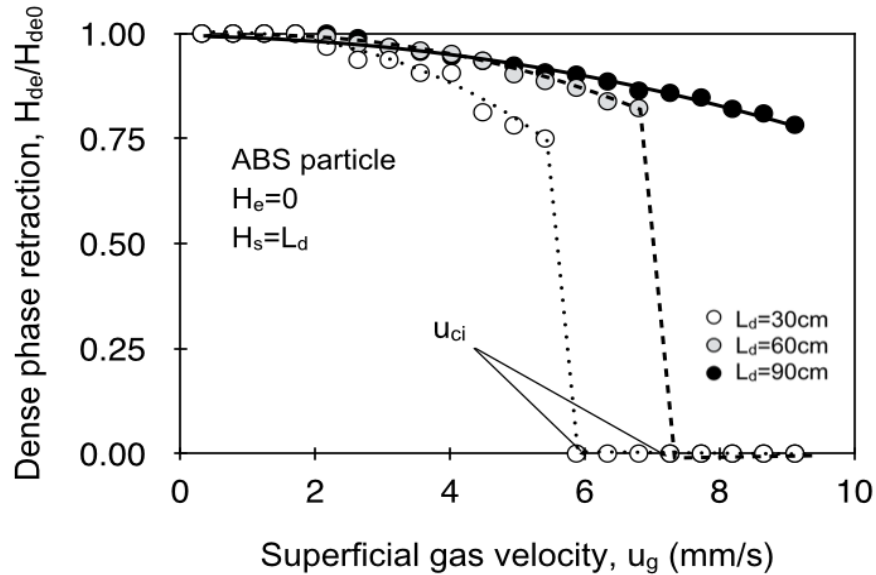


Figure 2.14 Effect of draft tube length on minimum circulating velocity

2.5.2 Nozzle-tube gap

The nozzle-tube gap is the distance between the bottom of the draft tube and top of the gas nozzle. It has been proven that the particle velocity in the annulus region increases with larger nozzle-tube gap in gas-solid systems (Zhao et al. 2006). Therefore, the impact of the nozzle-tube gap is studied in this work for the gas-driven gas-liquid-solid spouted bed.

The full spouting velocities for different nozzle-tube gaps are approximately the same, as shown in Figure 2.15. This is because equal amounts of solids require the same superficial gas velocity to break the loose-packed bed and the solids in the annulus can compensate for the spouting region. In addition, the slopes of these three lines vary, indicating that higher nozzle-tube gap group leads to higher particle velocity in the annulus. This phenomenon may be due to some gas leaks into the annulus region. The leaking gas occupies space in the annulus as the buoyancy force of water decreases. This phenomenon strengthens the gravity force on the particles in the annulus and

allowing the particles to settle more quickly. In addition, a higher nozzle-tube gap provides more space for particles to cross from the annulus to the spouting region, increasing the particle velocity. This phenomenon has also been observed in a gas-solid system (Berruti et al., 1988; Zhao et al., 2006).

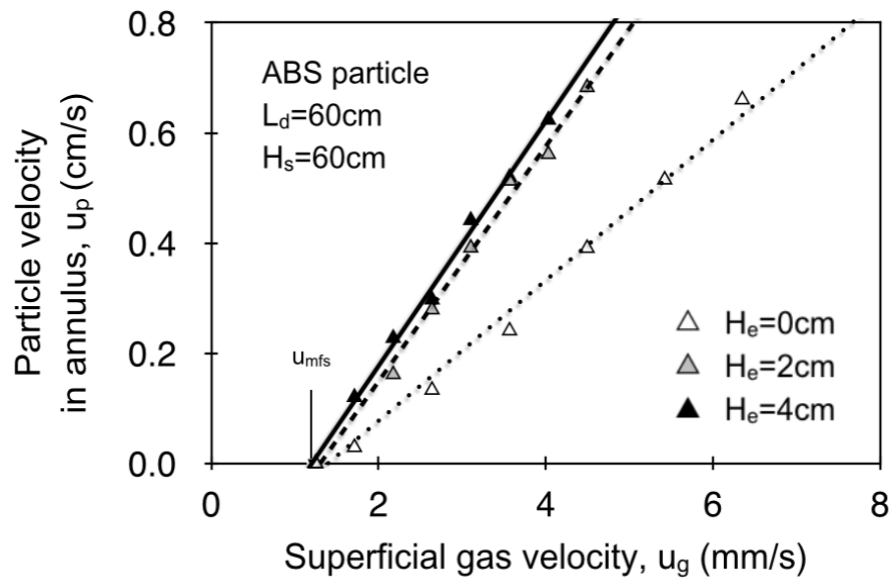


Figure 2.15 Nozzle-tube gap effect on full spouting velocity

The minimum circulating velocity increases with decreasing nozzle-tube gap, as shown in Figure 2.16. This may be because the leaking gas in the annulus region and more space for higher gap cause the particles in the annulus region moving more quickly, as shown in Figure 2.15. Therefore, the quantity of particles in the annulus region decreases more rapidly for a longer nozzle-tube gap as it requires less superficial gas velocity increasing to change to a internal circulating bed.

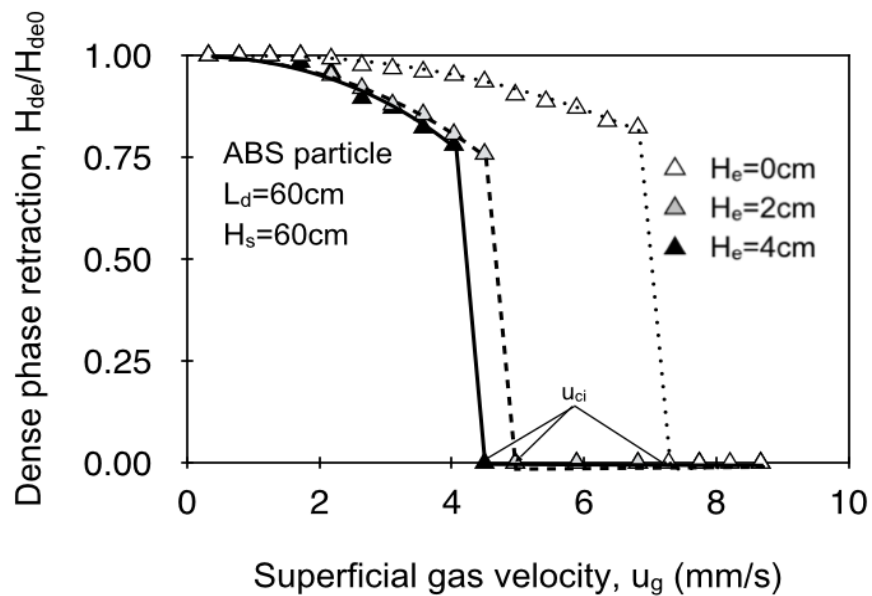


Figure 2.16 Nozzle-tube gap effect on minimum circulating velocity

2.5.3 Particle density

The minimum spouting velocity increases with increasing particle density, as shown in Figure 2.17. This phenomenon is due to the particles with higher density being more difficult to spout as they are heavier, requiring a higher superficial gas velocity to provide the necessary drag force to break the loose-packed bed.

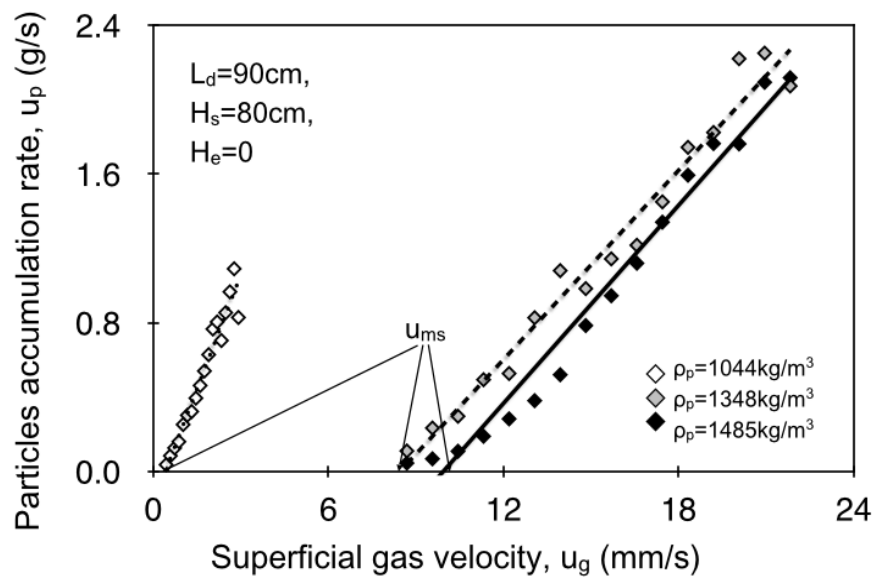


Figure 2.17 Particle density effect on minimum spouting velocity

The full spouting velocity increases with increasing particle density, as shown in Figure 2.18. This is because the particle with higher density is harder to spout as explained in Figure 2.17. The particles require a higher superficial gas velocity to begin circulation. Additionally, the fountain is smaller for a particle with higher density, resulting in the particles located in fountain falling back to the annulus more quickly. The particle circulation development from the central

annulus to the column wall is thus slower. The semi circulation solids flow pattern can be better maintained so that the particles close to wall are more difficult to move.

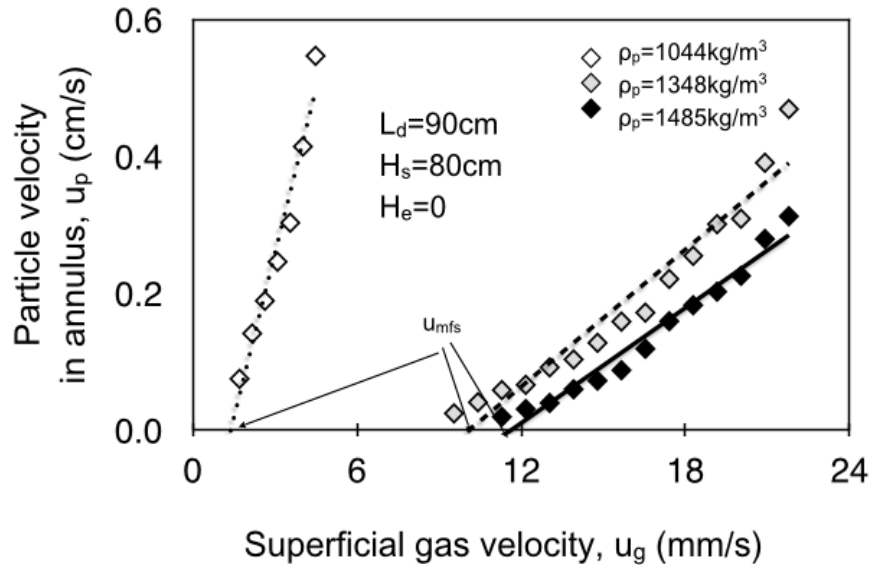


Figure 2.18 Particle density effect on full spouting velocity

The minimum circulating velocity increases with particle density, as shown in Figure 2.19. It is evident that the particle with higher density have slower dense phase retraction, indicating the particles with higher density has a higher minimum circulating velocity. This is because both the minimum spouting velocity and full spouting velocity are higher for a particle with higher density, as explained in Figure 2.17 and Figure 2.18. The particles are harder to spout and settle more easily. Therefore, the dense phase height in the annulus requires higher superficial gas velocity to retract.

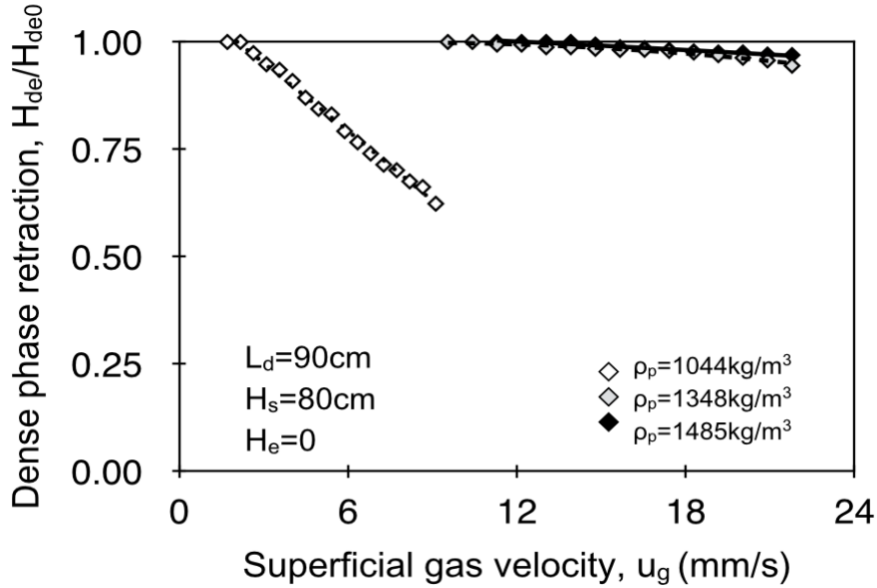


Figure 2.19 Particle density effect on minimum circulating velocity

2.6 Particle accumulation rate measurement

Two methods were used to estimate particle accumulation rate in this work, the basket method and an estimate based on the particle velocity in the annulus region. The basket can directly measure how weight particles accumulates in the annulus, while the estimate from the particle velocity is based on measurements at the wall of the column. The particle and particle velocity distribution are assumed to be uniform in the radial and vertical directions when the spouted bed achieves full spouting regime. In addition, the voidage in dense phase in the spouting regime is assumed to be the same as the packed bed. The particle accumulation rate can thus be calculated in the basket (w_{pb}) using Equation 2.7:

$$w_{pb} = u_p \times \frac{\pi}{4} \times (D_i^2 - D_t^2) \times \rho_b \times \frac{\frac{\pi}{4} \times D_b^2}{\frac{\pi}{4} \times (D_i^2 - D_t^2)} \quad (2.7)$$

Equation (2.7) can be simplified to Equation (2.8)

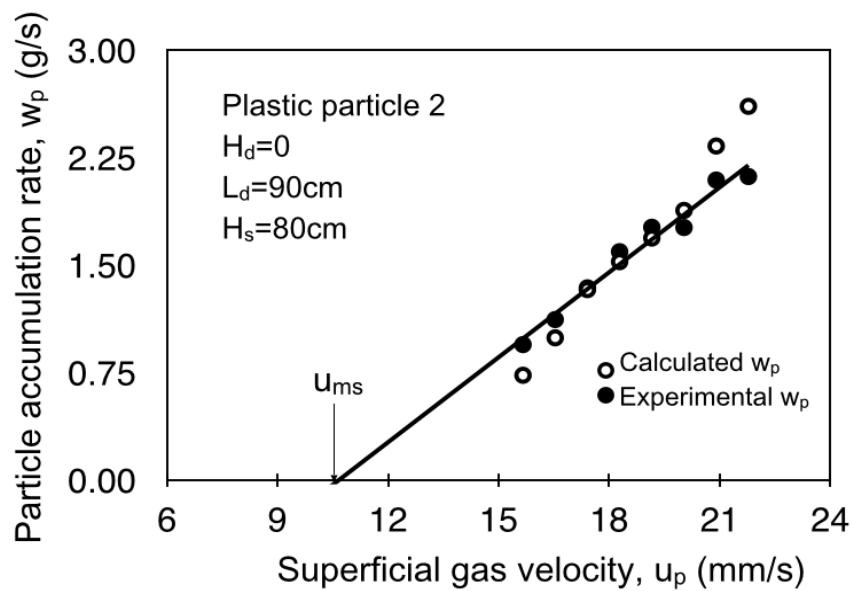
$$w_{pb} = \frac{\pi u_p \rho_b D_b^2}{4} \quad (2.8)$$

In Equation 2.7 and 2.8, w_{pb} is the particle mass accumulation rate in the basket, u_p is the particle moving velocity in annulus, ρ_b is the particle density, D_b is the inner diameter of basket.

The set of data for the plastic particles 2 were selected to study the particle accumulation rate (w_p) comparison between the basket method and the calculation from the particle velocity in the annulus region at wall, as shown in Figure 2.20. The calculated values are lower in the low superficial gas velocity region. This may be because the particle velocity in the central annulus region is higher than that at wall (Schlichting & Gersten, 2017; He et al., 1994), causing the calculation value to be smaller than the actual value. In the high superficial gas velocity region, the calculation rate is larger than the basket method. This may be because the dense phase in the annulus region becomes looser when the superficial gas velocity is high (He et al., 1994; Pianarosa et al., 2000), meaning the bulk density is higher than the dense phase density in the annulus region. Therefore, the calculation value is higher than the actual value. The minimum spouting velocity under this operating condition is 11 mm/s as shown in Figure 2.20. The deviation between the calculation particle accumulation rate in the basket and experimental particle accumulation rate in the basket is smaller than 10% as shown in Table 2.4, which shows that the particle circulation rate can be roughly calculated by the particle downward velocity in the superficial gas velocity range from $1.5u_{ms}$ to $1.8u_{ms}$.

Table 2.4 Deviation of calculated and experimental w_p

Superficial gas velocity (mm/s)	15	16	17	18	19	20	21	22
Calculated w_p (g/s)	0.731	0.992	1.329	1.523	1.688	1.881	2.331	2.607
Experimental w_p (g/s)	0.945	1.120	1.341	1.593	1.764	1.762	2.093	2.118
Relative deviation	-22.6%	-11.4%	-0.9%	-4.4%	-4.3%	6.8%	11.3%	23.1%

**Figure 2.20 Comparison of experimental particle accumulation and calculated particle accumulation in basket**

2.7 Summary

- The designed experimental gas-driven gas-liquid-solid spouted bed was successfully operated with the ABS particle, plastic particle 1 and plastic particle 2.
- In the gas-driven gas-liquid-solid spouted bed, the spouted bed flow regimes were observed to transition from fixed bed, semi spouted bed, full spouted bed and internal circulating fluidized bed with increasing gas velocity. The regime transition velocities respectively are minimum spouting velocity, full spouting velocity and minimum circulating velocity.
- The minimum spouting velocity, full spouting velocity and minimum circulating velocity all increased with increasing draft tube length and particle density. The minimum spouting velocity and full spouting velocity are not functions of nozzle-tube gap. The minimum circulating velocity increased with decreasing nozzle-tube gap.
- The particle accumulation rate can be roughly estimated by calculation methods using particle moving velocity at wall when superficial velocity is in the range of $1.5u_{ms}$ to $1.8 u_{ms}$.

References

Anabtawi, M., Hilal, N., Al Muftah, A., & Leaper, M. (2003). Volumetric mass transfer coefficient in non-Newtonian fluids in spout fluid beds. *Chemical Engineering Technology*. **26**, 759-764

Bi, X. (2011). *Initiation of spouting*. Chapter 2 of *Spouted and Spout-fluid Beds* edited by Epstein, N., & Grace, J. Cambridge, London, UK

Berruti, F., Muir, J., & Behie, L. (1988). Solids circulation in a spout-fluid bed with draft tube. *The Canadian Journal of Chemical Engineering*. **66**, 919-923

Epstein, N., & Grace, J. (2011). *Introduction*. Chapter 1 of *Spouted and Spout-fluid Beds* edited by Epstein, N., & Grace, J. Cambridge, London, UK

Erbil, A. (2005). Effect of the annulus aeration on annulus leakage and particle circulation in a three-phase spout-fluid bed with a draft tube. *Powder Technology*. **162**, 38-49

Gokon, N., Takahashi, S., Yamamoto, H., & Kodama, T. (2008). Thermochemical two-step water-splitting reactor with internally circulating fluidized bed for thermal reduction of ferrite particles. *International Journal of Hydrogen Energy*. **33**, 2189-2199

Grbavcic, Z., Littman, H., & Morgan, M. (2011). *Liquid and liquid-gas spouting of solids*. Chapter 20 of *Spouted and Spout-fluid Beds* edited by Epstein, N., & Grace, J. Cambridge, London, UK

Grbavcic, Z., Vukovic, D., Jovanovic, S., Garic, R., Hadzismajlovic, D., Littman, H., & Morgan, M. (1992). Fluid flow regime and solids circulation rate in a liquid phase spout-fluid bed with draft tube. *The Canadian Journal of Chemical Engineering*. **70**, 895-904

He, Y., Lim, C., & Grace, J., & Zhu, J. (1994). Measurements of voidage profiles in spouted beds. *The Canadian Journal of Chemical Engineering*. **72**, 561-568

He, Y., Qin, S., Lim, C., & Grace, J. (1994). Particle velocity profiles and solid flow regimes in spouted beds. *The Canadian Journal of Chemical Engineering*. **72**, 561-568

Khan, A., & Richardson, J. (1989). Fluid-particle interactions and flow characteristics of fluidized beds and settling suspensions of spherical particles. *Chemical Engineering Communications*. **78**, 111-130

Littman, H., Vukovic, V., Zdanski, F., & Grbavcic, Z. (1974). Pressure drop and flowrate characteristics of a liquid phase spout-fluid bed at the minimum spout-fluid flowrate. *The Canadian Journal of Chemical Engineering*. **52**, 174-179

Markowski, A., & Kaminski, W. (1983). Hydrodynamic characteristic of jet-spouted beds. *The Canadian Journal of Chemical Engineering*. **61**, 377-381

Mathur, K., & Gisher, P. (1955). A study of the application of the spouted bed technique to wheat drying. *Journal of Applied Chemistry*. **5**, 624-636

Pianarosa, D., Freitas, L., Lim, C., Grace, J., & Dogan, M. (2000). Voidage and particle velocity profiles in a spout-fluid bed. *The Canadian Journal of Chemical Engineering*. **78**, 132-142

Schlichting, H. & Gersten, K. (2016). *Boundary-Layer Theory*. Berlin, Heidelberg, Germany

Vukovic, D., Zdanski, F., Vunjak, G., Grbavcic, Z., & Littman, H. (1974). Pressure drop,

bed expansion, and liquid holdup in a three-phase spouted bed contactor. *The Canadian Journal of Chemical Engineering*. **52**, 180-184

Wang, J., Wang, T., Liu, L., & Chen, H. (2003). Hydrodynamics behavior of a three-phase spouted bed with very large particles. *The Canadian Journal of Chemical Engineering*. **81**, 861-866

Zhao, X., Yao, Q., & Li, S. (2006). Effects of draft tubes on particle velocity profiles in spouted beds. *Chemical Engineering Technology*. **7**, 875-881

Chapter 3

3 Hydrodynamics in Gas-Driven Gas-Liquid-Solid Spouted Bed without a Draft Tube

3.1 Background information

Conventional gas-solid spouted bed was first proposed by Mathur and Gisher in 1950s for grain drying process (Mathur & Gisher, 1955). Gradually, this configuration start seeing use in other chemical engineering processes, including solids blending, gas cleaning and thermal cracking (Markowski & Kaminski, 1983). A conventional gas-solid spouted bed is a fluidized bed reactor that contacts particles and a fluid in a well-mixed regime. The configuration consists of a cylindrical vertical column filled with particles where fluid is injected from a nozzle at the center of the column bottom (Epstein & Grace, 2011), as illustrated in Figure 3.1. The injected fluid provides drag force and buoyancy force to bring particles upwards at the center of the column (Epstein & Grace, 2011), which then break through the static bed and fall back down due to gravity, resulting in the solids circulation regime (Epstein & Grace, 2011).

In gas-solid spouted bed, there are four regions in a stable spouted bed including spouting region, annulus region, fountain region and dead zone (Zhu & Hong, 1997). The region where particles move upwards is the spouting region, while the region where particles flow down is referred as the annulus region. The particles above the spouting region and annulus region is fountain region. In this region, particles shift movement from rising to falling. In a flat bottom bed, a dead zone is naturally formed at the bottom as the particles in this region cannot be removed by both gas flow and gravity.

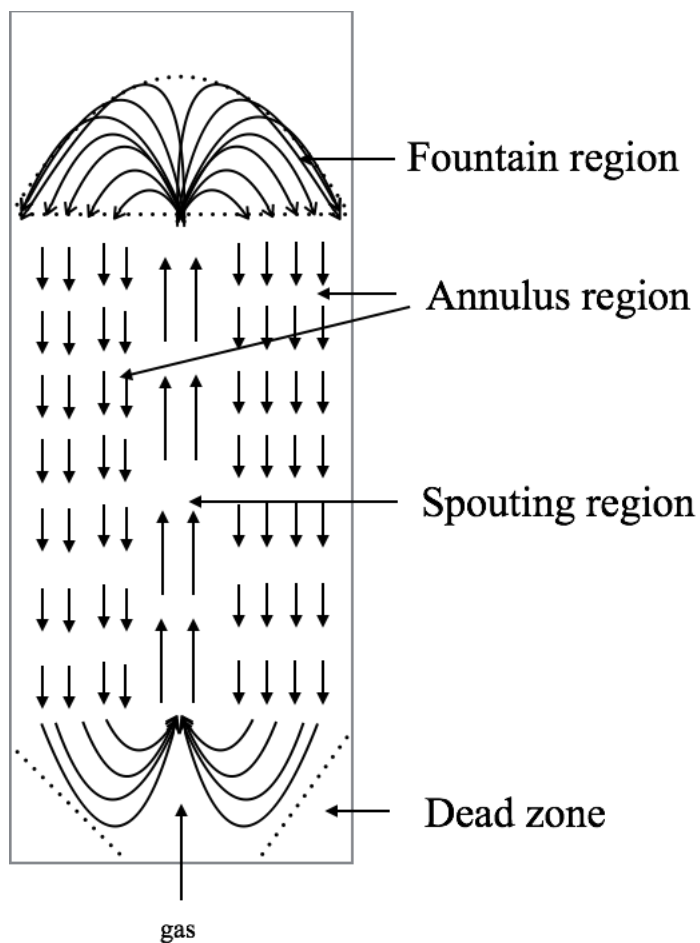
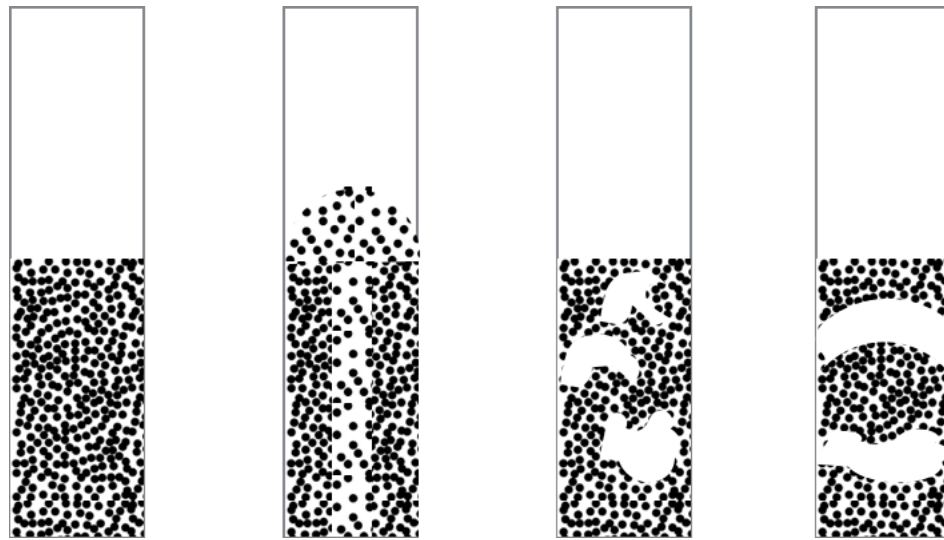


Figure 3.1 Schematic diagram of a spouted bed. Arrows indicate direction of solids motion.

Figure 3.2 illustrates the four regimes in transitional gas-solid spouted bed without a draft tube including fixed (packed) bed, spouted bed, bubbling bed and slugging bed, which can occur in a spouted bed with increasing gas superficial velocity (Epstein & Grace, 2011). However, fixed packed bed may directly change from fixed bed into a bubbling bed and a stable spouted bed cannot be developed when the initial static bed height is higher than the maximum spoutable height of this system (Yang, 2003). Gas leakage from the spouting region to the annulus region can fluidize the particles in the annulus region and breaks the spouting regime.



(a) Fixed bed (b) Spouted bed (c) Bubbling bed (d) Slugging bed

Figure 3.2 Flow regime transition with increasing gas flow

To adopt the spouted bed in other phase systems for wider application, some researchers developed other non-conventional types of spouted bed such as the liquid-solid spouted bed (Grbavcic et al., 1992) and liquid-driven gas-liquid-solid spouted bed (Wang et al. 2003). However, little research has been completed for gas-driven gas-liquid-solid spouted bed, in which uses gas only to form spout without liquid net flow.

Gas-liquid-solid spouted beds have a high potential to be used in wastewater treatment processes such as the aeration process unit. In this application, gas-driven systems are better as the energy input to spout particles can be provided by the aeration gas so that there is no need to recirculate the liquid to form spouting. In this system, gas is injected from the central bottom of the column, which is filled with particles and stagnant water. The fluid provides drag force and buoyancy force for the particles and they are able to move upwards in the central region. Next, the particles break through the loose packed bed and fall down into the surrounding region. It can be divided into four regions similarity to the gas-solid spouted bed, as shown in Figure 3.1.

The previous work has proven that the gas-driven gas-liquid-solid spouted bed is feasible with a draft tube, as shown in Chapter 2. Therefore, this work is aimed to construct a gas-driven gas-liquid-solid spouted bed without a draft tube to compare with the spouted bed with a draft tube. In addition, the dead zone length at the wall is studied to maximize the useful particle volume and its practicality for design of a conical bottom. It has been proven that the dead zone length is a function of initial static bed height and gas flowrate in gas-solid spouted beds (Jose, 1996). Therefore, the gas initial static bed height and gas flowrate are investigated in this work. Furthermore, water level is also studied to find its effect.

3.2 Experimental apparatus and methods

3.2.1 Experimental apparatus

Figure 3.3 shows the experimental system used for this work. Water and air are used in the liquid and gas phases, respectively. The vertical column is filled with particles and water, and is constructed of transparent plexiglass with a 152 mm (6 inch) inner diameter (D_i) and 6 mm thickness, while open to the atmosphere. A gas injection nozzle with an inner diameter (d_n) of 4.5 mm and 1 mm thickness is located at the center of the column bottom. Three initial static bed heights (H_s) (300mm, 450mm and 600mm), five water levels higher than the static bed heights (H_w) (0, 50mm, 200mm, 400mm, 600mm) and three gas flowrates (Q_g) (2.23 l/min, 4.46 l/min, 8.93 l/min under ambient pressure) were studied to investigate their effects on key hydrodynamic characteristics.

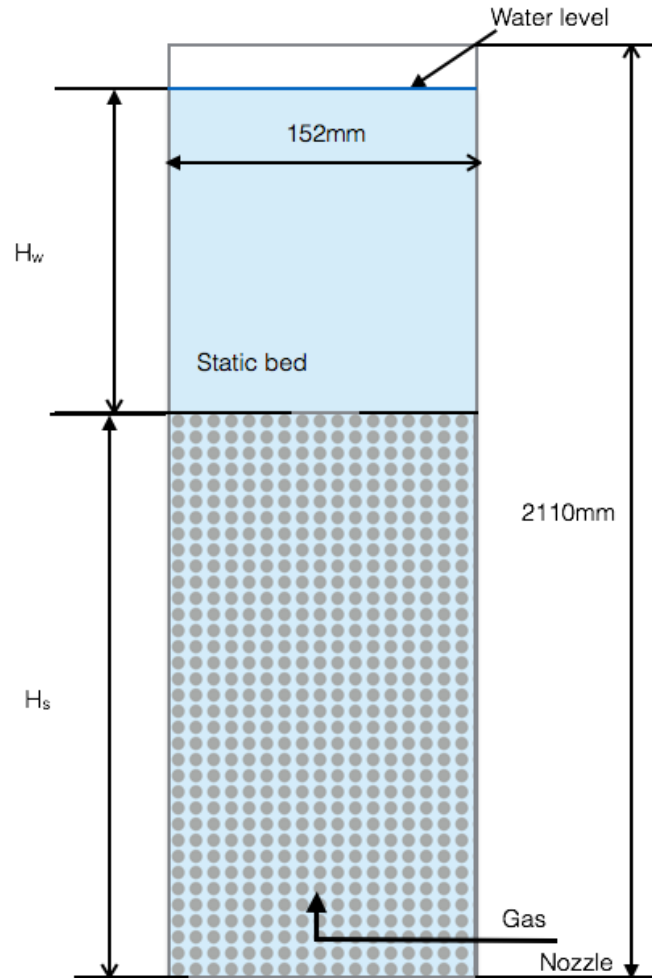


Figure 3.3 Apparatus of gas-driven gas-liquid-solid spouted bed without draft tube

3.2.2 Particle properties

Three kinds of particles including Acrylonitrile Butadiene Styrene (ABS) plastic particle and other two kinds plastic particles were used to try to form a spouting regime. Their properties are shown in Table 3.1

Table 3.1 Properties of particle

Particle Type	Particle Density (kg/m ³)	Bulk Density (kg/m ³)	Volume Equivalent Diameter (mm)	Archimedes Number	Terminal Velocity in Liquid (m/s)
ABS plastic particle	1044	644	2.5	6737.5	0.036
plastic particle1	1348	803	0.7	1170	0.011
plastic particle2	1485	819	1.5	15711	0.062

Archimedes number and terminal velocities are calculated by Equation 3.1, 3.2 and 3.3 (Khan & Richardson, 1988)

$$Ar = \frac{3}{4} C_{Dt} Re_t^2 = d_p^3 \rho (\rho_s - \rho) g / \mu^2 \quad (3.1)$$

$$Re_t = (2.33Ar^{0.018} - 1.53Ar^{-0.016})^{13.3} \quad (3.2)$$

$$u_t = \frac{\mu Re_t}{d_p \rho_p} \quad (3.3)$$

3.2.3 Methods

The dead zone length (L_n), illustrated in Figure 3.4, was measured based on visual observations at the wall. The reported dead zone length subtracts the height below the nozzle exit level. The interface between the annulus region and the dead zone is identified based on the highest particle which does not move over a 30 seconds period. Each group of experiments was measured three times and the average values of each group is used. Results are reported based on the gas

flowrate because there is no clear interface between the spouting region and annulus region, as shown in Figure 3.4. The cross-sectional surface area for gas flow thus cannot be readily defined.

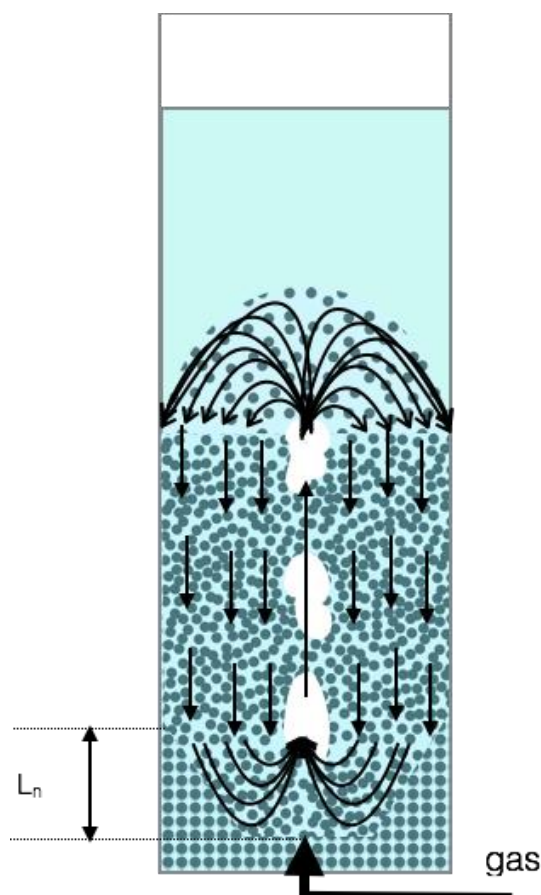


Figure 3.4 Particle motion and dead zone at wall above the nozzle exit level (Arrows indicate particle motion)

3.3 Result and discussion

3.3.1 Attempt of spouting regime construction

Three particles were tested in a gas-driven gas-liquid-solid spouted bed configuration. Only the ABS plastic particles successfully formed a spouting flow regime for the studied operating conditions in this work (initial bed height range from 300mm to 600mm; water level higher than initial static bed rang from 0 to 600mm; gas flowrate range from 2.23 l/min to 8.93 l/min). The

observed flow regimes of the other two particles directly changes from packed bed to fluidized bed. This is because these two types of particles have smaller size, which are easy to be fluidized (Koide et al., 1983) and can be suspended in the liquid phase even with a poor gas distributor (nozzle). The gas readily leaks from the spouting region to the annulus region, thus suspending the particles. This prevents the particles in the annulus from falling down and the spouting flow pattern.

Unlike these two kinds of particles, ABS particle has bigger size, which can be readily form a spouted bed. The spouting regime formed by ABS particles, however, can be stopped by elevated gas flowrates. Instead of changing to an internal circulating fluidized bed region like the spouted bed with draft tube, the regime changes to a fluidized bed. This is because the leaking gas flow fluidizes the particles in the surrounding region hence a circulating regime is broken. This phenomenon only occurred in this work in the 30cm initial static bed height with 8.93 l/min gas flowrate and 60cm water level group.

3.3.2 Effect of gas flowrate on dead zone length

Figure 3.5 shows that the dead zone length at the wall above the nozzle exit level decreases with increasing gas flowrate. Similar trends have been observed in a gas-solid spouted bed (Jose et al., 1996). This may be because the higher gas flowrate drives water in the spouting region to move quicker so that the water in the annulus region moves downwards quicker, providing a stronger drag force. The original non-mobile particles in the dead zone, which is near the interface between annulus region and dead zone, thus begin moving and decrease the dead zone length.

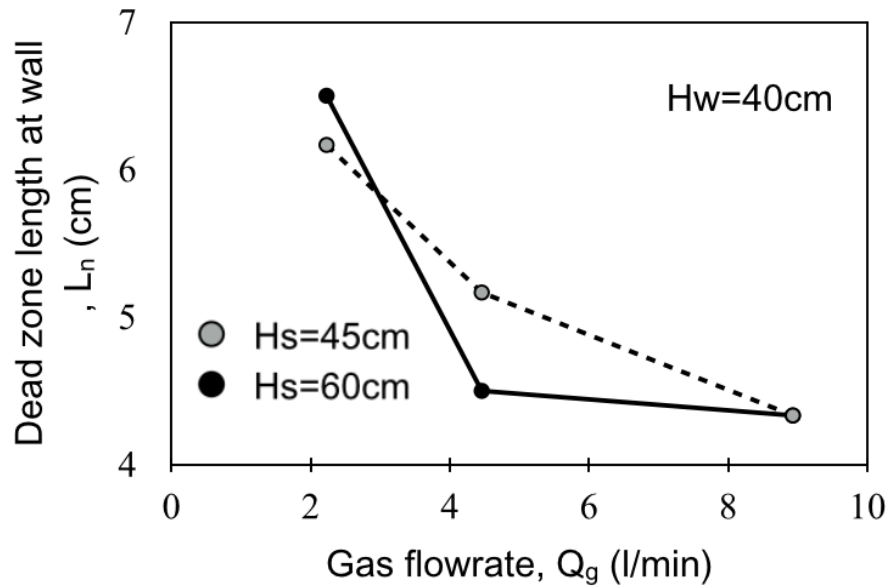


Figure 3.5 Dead zone length variance with gas flowrate (ABS particle)

3.3.3 Effect of initial static bed height on dead zone length

Figure 3.6 shows that the dead zone length decreases when the initial static bed is increased. This phenomenon may be because a more vigorous movement, such as slugging, takes place at the bottom of spouted bed when the initial static bed height is higher (Jose et al, 1996). The slugging provides stronger drag force to the particles in the surrounding region. Therefore, some non-mobile particles at top of the dead zone can be spouted upwards and begin circulation. The dead zone length at wall decreases as a result.

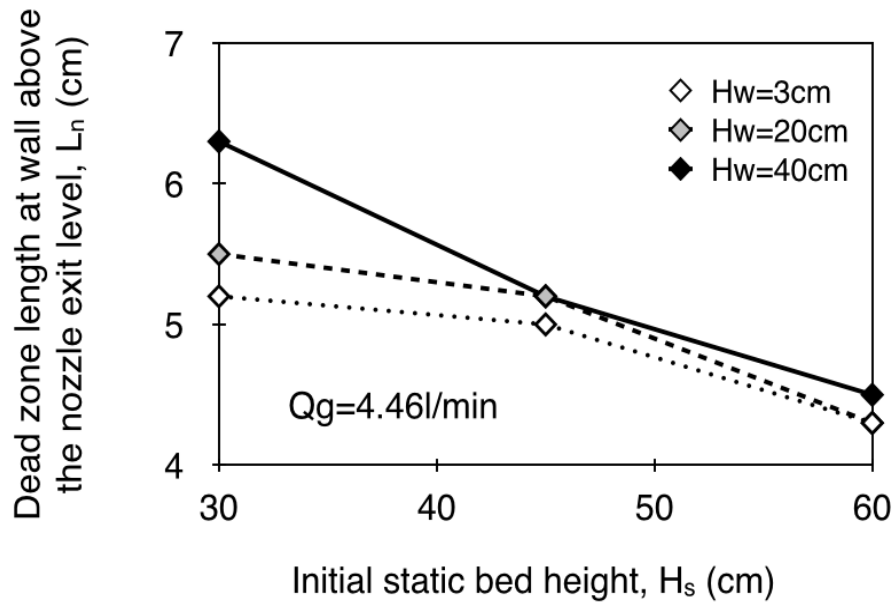
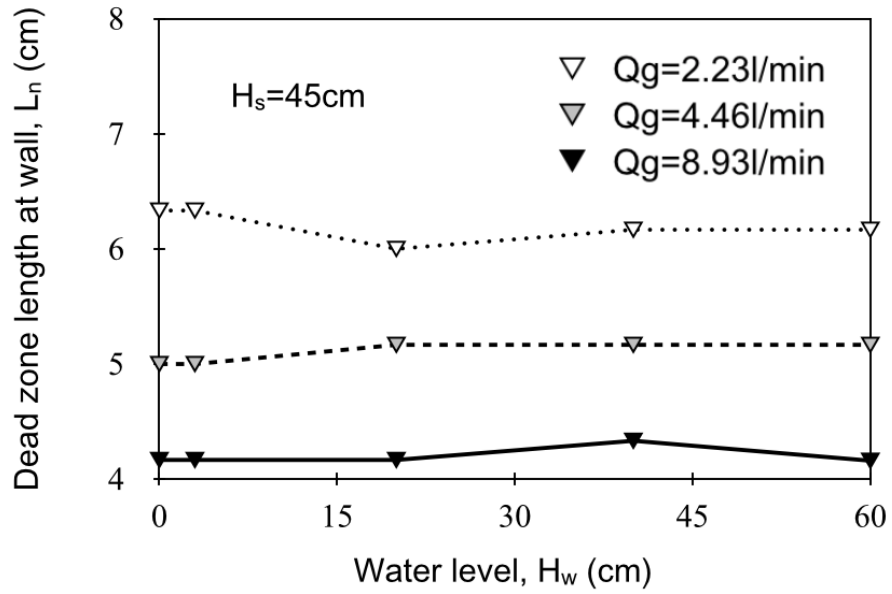


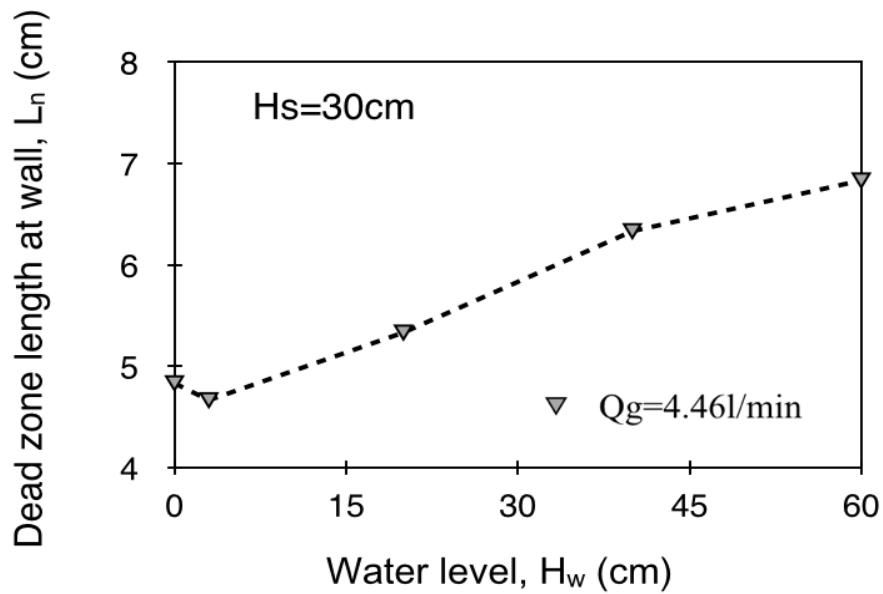
Figure 3.6 Dead zone length variance with initial static bed height (ABS particle)

3.3.4 Effect of water level on dead zone length

Figure 3.7 (a) shows that the dead zone lengths at wall are approximately the same for the studied water levels when the initial static bed height is 45 cm. It is believed that the gas flow motion and distribution are similar for different water levels, which means the fluid provides comparable drag force. However, the dead zone length at wall increases with water level when initial static bed height is 30 cm, as shown in Figure 3.7 (b). This may be because the particle quantity is lower. The system is thus easier to transition from spouted bed to fluidized bed, especially when the water level is higher because water can provide more space for the particles to be suspended. It is believed that this system has a larger dead zone when it converts to a fluidized bed because the nozzle is a bad distributor. Therefore, the dead zone length increases with water level when the initial static bed height is low.



(a)



(b)

Figure 3.7 Dead zone length variance with water level (a) $H_s=45$ cm, (b) $H_s=30$ cm (ABS particle)

3.4 Summary

- A gas-driven gas-liquid-solid spouted bed without draft tube was formed with ABS particles. However, the other two types of particles cannot be used to form a spouting regime.
- The regime transition after the spouting bed is the fluidized bed, not the internal circulating fluidized bed.
- Dead zone length decreases with increasing gas flowrate and initial static bed height. In addition, it is not influenced by water level. However, the dead zone length increases if the system changes to fluidized bed.

Reference

Berruti, F., Muir, J., & Behie, L. (1988). Solids circulation in a spout-fluid bed with draft tube. *The Canadian Journal of Chemical Engineering*. **66**, 919-923

Epstein, N., & Grace, J. (2011). *Introduction* Chapter 1 of *Spouted and spout-fluid beds* edited by Epstein, N. & Grace, J., Cambridge, UK

Grbavcic, Z., Vukovic, D., Jovanovic, S., Garic, R., Hadzismajlovic, D., Littman, H., & Morgan, M. (1992). Fluid flow regime and solids circulation rate in a liquid phase spout-fluid bed with draft tube. *The Canadian Journal of Chemical Engineering*. **70**, 895-904

Jose, M., Olazar, M., Llamosas, R., Izquierdo, M., & Bilbao, J. (1996). Study of dead zone and spout diameter in shallow spouted beds of cylindrical geometry. *The Chemical Engineering Journal*. **64**, 353-359

Koide, K., Horibe, K., Kawabata, H., & Ito, S. (1983) Critical gas velocity required for complete suspension of solid particles in solid-suspended bubble column with draught tube. *Journal of Chemical Engineering of Japan*. **17**, 368-374

Markowski, A., & Kaminski, W. (1983). Hydrodynamic characteristic of jet-spouted beds. *The Canadian Journal of Chemical Engineering*. **61**, 377-381

Pianarosa, D., Freitas, L., Lim, C., Grace, J., & Dogan, M. (2000). Voidage and particle velocity profiles in a spout-fluid bed. *The Canadian Journal of Chemical Engineering*. **78**, 132-142

Wang, J., Wang, T., Liu, L., & Chen, H. (2003). Hydrodynamics behavior of a three-phase

spouted bed with very large particles. *The Canadian Journal of Chemical Engineering*. **81**, 861-866

Yang, W. (2003). *Other nonconventional fluidized beds*, Chapter 20 of *Handbook of Fluidization and Fluid-Particle systems edited by Yang, W.*. Pittsburgh, Pennsylvania, USA

Zhu, J., & Hong, J. (1997). Development and current status of research on spouted bed. *Chemical Reaction Engineering and Technology*. **13**, 207-230

Chapter 4

4 Conclusions and Future Work

4.1 Conclusions

In this research project, a novel gas-driven gas-liquid-solid spouted bed was successfully developed. In the spouted bed with a draft tube, four flow regimes were identified and three regime transition velocities in between were defined and studied. A new “basketing method” was adopted to measure the minimum spouting velocity, while monitoring the particle velocity and the dense phase retraction was used to determine the full spouting velocity and minimum circulating velocity, respectively. The internal solids circulation rate was also estimated by two different methods and the results were successfully compared. In the spouted bed without draft tube, dead zone length at wall was also studied.

All three types of particles can be successfully spouted in the gas-driven gas-liquid-solid spouted bed with a draft tube. This system has four regions including spouting region, annulus region, fountain region and dead zone region, the same as the traditional gas-solid spouted bed. For system operation, there are four regimes found, fixed bed, semi spouted bed, full spouted bed and internal circulating fluidized bed. The velocities for the regime transitions are minimum spouting velocity, full spouting velocity and minimum circulating velocity. These three velocities increase with increasing draft tube length. It is also found that the nozzle-tube gap does not affect the minimum spouting velocity and full spouting velocity, but the minimum circulating velocity is lower for a larger nozzle-tube gap. The three transition velocities are also found to increase with increasing particle density. Additionally, it is found that the particle accumulation rate can be roughly estimated by the particle velocity in the annulus when the superficial gas velocity is in range between $1.5 u_{ms}$ to $1.8 u_{ms}$.

Without a draft tube, only ABS plastic particle could be successfully spouted. The effect of operating conditions on dead zone length were studied. The dead zone length at wall is not significantly affected by the water level, but reduces with increasing gas flowrate and initial static bed height.

4.2 Future Work

A two-dimension or semi-cylindrical bed can be used to study the inner particle motion in this new type of spouted bed. To better analyze the effect of particle density, particles with the same diameter but different densities should be tested in future work. Particle with different shapes can be also studied. Additionally, effect of nozzle diameter can also be examined in relation to the transition velocities. More types of particles can also be evaluated for their possible application in the gas-driven gas-liquid-solid spouted bed without the draft tube.

Appendices

Appendix A. Example of error analysis

Plastic particle 2 with 90cm draft tube, 0cm H_e and 80cm initial static bed was chosen to repeat six times in particle accumulation rate measurement to prove that the latter part of particle accumulation rate is proportional with gas flowrate. Figure A. shows the average value and error bar of this group. R^2 is very close to 1. These two factors demonstrate high correlation.

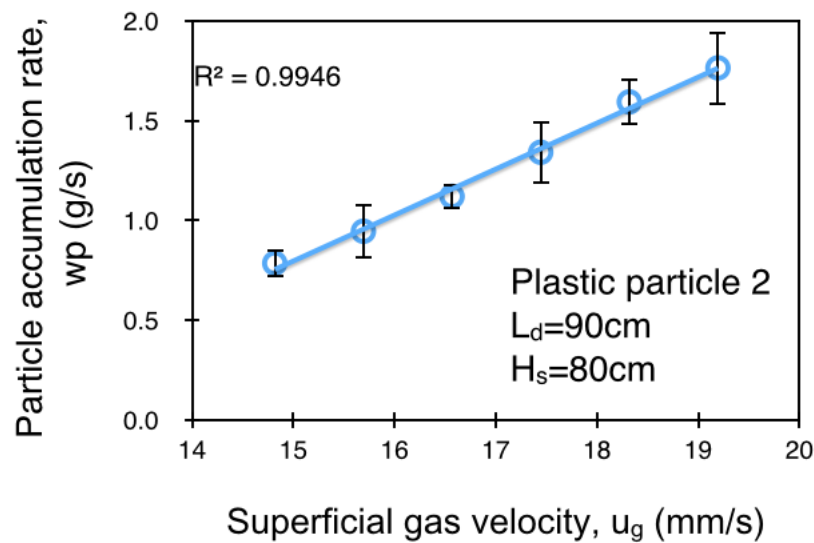


Figure A. Particle accumulation rate versus gas superficial velocity with error bar for plastic particle 2 with a 90cm draft tube and 80cm static bed height.

Every group studied the particle moving velocity in annulus region versus gas superficial velocity was repeated three times. Figure B shows the error bar chart of the ABS plastic particle moving velocity in the annulus region with a 90cm draft tube and 90cm initial static bed. R^2 is very close to 1. These two factors are highly correlated.

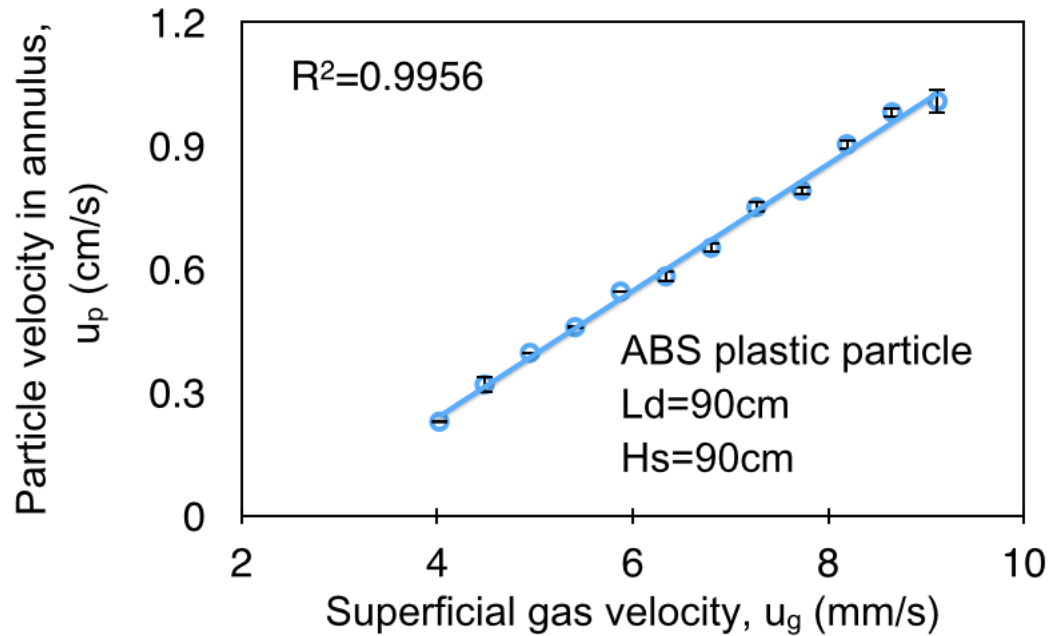


Figure B. Particle moving velocity in annulus region versus gas superficial velocity with error bar for ABS plastic particle with a 90cm draft tube and 90cm static bed height.

Every groups for dead zone length measurement was repeated three times. Figure C shows the error bar chart of an example group.

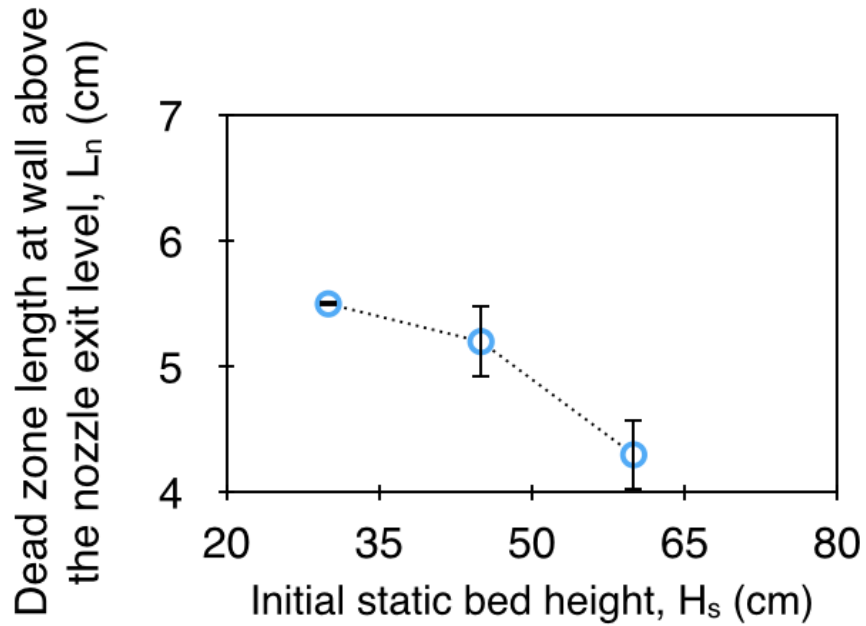
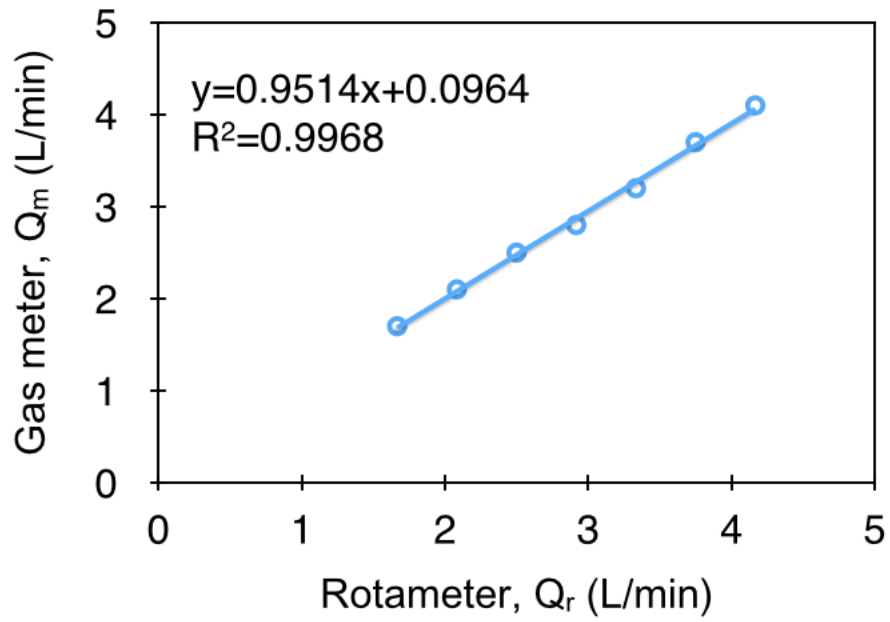


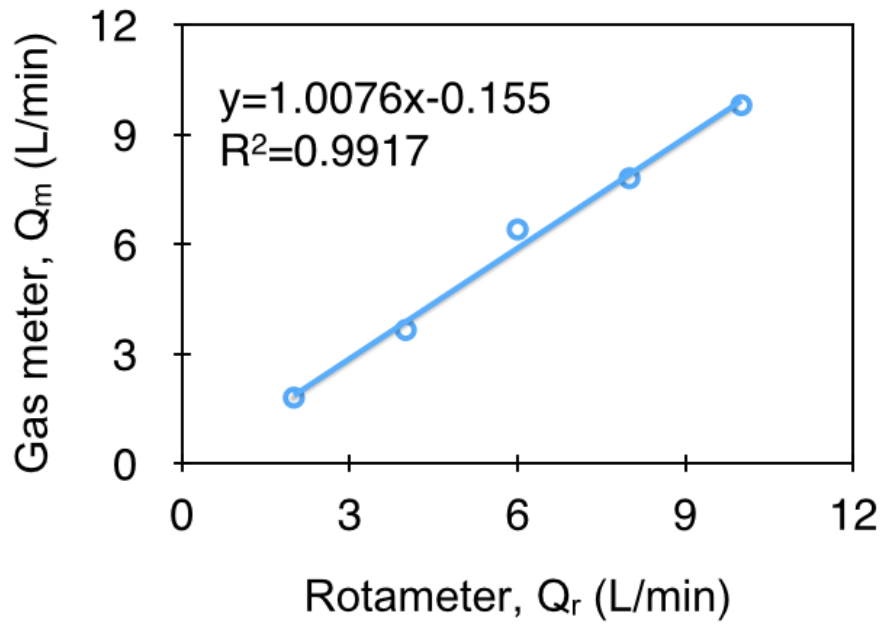
Figure C. Dead zone length versus initial static bed height with error bar for ABS plastic particle with 20cm water level and 4.46 l/min gas flowrate

Appendix B. Rotameter calibration

Two rotameters were used in this project. They are calibrated by a gas meter under atmosphere pressure. Figure C. (a), (b) shows the calibration curve used to determine the real gas flowrate directly from rotameter.



(a)



(b)

Figure C. Rotameter calibration curves, (a) rotameter 1; (b) rotameter 2

Appendix C. Data of experiments

Data of particle accumulation rate

ABS plastic particle, $H_e=0$ $L_d=30\text{cm}$, 60cm , 90cm , $H_s=L_d$

L_d (cm)	30	60	90
Superficial velocity in draft tube (mm/s)	Particle accumulation rate (g/s)		
0.00			
0.44	0.22	0.13	
0.59	0.25	0.17	0.01
0.73	0.30	0.23	0.07
0.88	0.28	0.22	0.16
1.02	0.42	0.34	0.27
1.17	0.57	0.38	0.45
1.32	0.56	0.54	0.35
1.46	0.69	0.46	0.52
1.61	0.74	0.52	0.46
1.75	0.84	0.51	0.53
1.90	0.85	0.64	0.68
2.05	0.86	0.67	0.75
2.19	1.00	0.76	0.83
2.34		0.99	0.76
2.48		0.81	0.70
2.63		1.04	0.87
2.78		0.96	0.87

Data of particle velocity in annulus

ABS plastic particle, $H_e=0$ $L_d= 60\text{cm}, 90\text{cm}$, $H_s=L_d$

L_d (cm)	60	90
Superficial velocity in draft tube (mm/s)	Particle moving velocity in annulus region (cm/s)	
1.25	0.00	0.00
1.71	0.05	0.02
2.18	0.13	0.05
2.64	0.16	0.10
3.10	0.20	0.14
3.57	0.31	0.19
4.03	0.36	0.23
4.50	0.44	0.32
4.96	0.54	0.40
5.42	0.60	0.46
5.89	0.66	0.55
6.35	0.72	0.58
6.82	0.77	0.65
7.28		0.75
7.74		0.79
8.21		0.90
8.67		0.98

Data of dense phase retraction in the annulus region

ABS plastic particle, $H_e=0$ $L_d=30\text{cm}, 60\text{cm}, 90\text{cm}$, $H_s=L_d$

L_d (cm)	30		60		90	
Superficial velocity in draft tube (mm/s)	Dense phase height (cm)	H_{de}/H_{de0}	Dense phase height (cm)	H_{de}/H_{de0}	Dense phase height (cm)	H_{de}/H_{de0}
0.3205	30.0	1.0000	60.0	1.0000	90.0	1.0000
0.7834	30.0	1.0000	60.0	1.0000	90.0	1.0000
1.2463	30.0	1.0000	60.0	1.0000	90.0	1.0000
1.7092	30.0	1.0000	60.0	1.0000	90.0	1.0000
2.1722	29.0	0.9688	59.5	0.9919	90.0	1.0000
2.6351	28.0	0.9375	58.5	0.9758	89.0	0.9891
3.0980	28.0	0.9375	58.0	0.9677	87.0	0.9674
3.5609	27.0	0.9063	57.5	0.9597	86.0	0.9565
4.0239	27.0	0.9063	57.0	0.9516	85.0	0.9457
4.4868	24.0	0.8125	56.0	0.9355	84.0	0.9348
4.9497	23.0	0.7813	54.0	0.9032	83.0	0.9239
5.4126	22.0	0.7500	53.0	0.8871	81.5	0.9076
5.8755	0	0	52.0	0.8710	81.0	0.9022
6.3385	0	0	50.0	0.8387	79.5	0.8859
6.8014	0	0	49.0	0.8226	77.5	0.8641
7.2643	0	0	0	0	77.0	0.8587
7.7272	0	0	0	0	76.0	0.8478
8.1901	0	0	0	0	73.5	0.8207
8.6531	0	0	0	0	72.5	0.8098
9.1160	0	0	0	0	70.0	0.7826

*Data of particle accumulation rate**ABS plastic particle, $L_d=60\text{cm}$, $H_s=L_d$, $H_e=0\text{cm}$, 2cm, 4cm*

H_e (cm)	0	2	4
Superficial velocity(mm/s)	Particle accumulation rate (g/s)	Particle accumulation rate (g/s)	Particle accumulation rate (g/s)
0.59	0.02		
0.73	0.14	0.01	
0.88	0.19	0.07	
1.02	0.23	0.09	0.05
1.17	0.31	0.17	0.20
1.32	0.38	0.21	0.30
1.46	0.34	0.32	0.33
1.61	0.44	0.29	0.42
1.75	0.44	0.46	0.47
1.90	0.58	0.52	0.57
2.05	0.47	0.54	0.64
2.19	0.56	0.51	0.70
2.34	0.79		0.70
2.48	0.61		0.67
2.63	0.84		0.76
2.78	0.76		0.75
2.92	0.97		0.80

Data of particle velocity in annulus

ABS plastic particle, $L_d=60\text{cm}$, $H_s=L_d$, $H_e=0\text{cm}$, 2cm , 4cm

H_e (cm)	Particle moving velocity in annulus region (cm/s)		
Superficial velocity(mm/s)	0	2	4
1.25	0.00	0.00	0.00
1.71	0.03		0.12
2.18		0.16	0.23
2.64	0.13	0.28	0.30
3.10		0.39	0.44
3.57	0.24	0.51	0.52
4.03		0.56	0.62
4.50	0.39	0.68	
4.96			
5.42	0.52		
5.89			

Data of dense phase retraction in the annulus region

ABS plastic particle, $L_d=60\text{cm}$, $H_s=L_d$, $H_e=0\text{cm}$, 2cm, 4cm

H_e (cm)	0		2		4	
Superficial velocity(mm/s)	Dense phase height (cm)	H_{de}/H_{de0}	Dense phase height (cm)	H_{de}/H_{de0}	Dense phase height (cm)	H_{de}/H_{de0}
0.32			60.0	1.0000	60.0	1.0000
0.78	60.0	1.0000	60.0	1.0000	60.0	1.0000
1.25	60.0	1.0000	60.0	1.0000	60.0	1.0000
1.71	60.0	1.0000	60.0	1.0000	59.0	0.9839
2.18	59.5	0.9919	57.0	0.9516	57.5	0.9597
2.64	58.5	0.9758	55.0	0.9194	53.5	0.8952
3.10	58.0	0.9677	52.5	0.8790	52.0	0.8710
3.57	57.5	0.9597	51.0	0.8548	49.0	0.8226
4.03	57.0	0.9516	48.0	0.8065	48.0	0.8065
4.50	56.0	0.9355	45.0	0.7581	0.0	0.0000
4.96	54.0	0.9032	0.0	0.0000	0.0	0.0000
5.42	53.0	0.8871	0.0	0.0000	0.0	0.0000
5.89	52.0	0.8710	0.0	0.0000	0.0	0.0000
6.35	50.0	0.8387	0.0	0.0000	0.0	0.0000
6.82	49.0	0.8226	0.0	0.0000	0.0	0.0000
7.28	0	0.0000	0.0	0.0000	0.0	0.0000
7.74	0	0.0000	0.0	0.0000	0.0	0.0000
8.21	0	0.0000	0.0	0.0000	0.0	0.0000
8.67	0	0.0000	0.0	0.0000	0.0	0.0000

*Data of particle accumulation rate**ABS plastic particle, plastic particle 1, plastic particle 2, $L_d=90\text{cm}$, $H_s=80\text{cm}$, $H_e=0\text{cm}$*

Particle density (kg/m^3)	1044	1348	1485
Superficial velocity(mm/s)	Particle accumulation rate (g/s)	Particle accumulation rate (g/s)	Particle accumulation rate (g/s)
0.44	0.04		
0.58	0.08		
0.73	0.13		
0.88	0.16		
1.02	0.25		
1.17	0.30		
1.31	0.32		
1.46	0.39		
1.60	0.46		
1.75	0.54		
1.90	0.63		
2.04	0.77		
2.19	0.80		
2.33	0.70		
2.48	0.85		
2.62	0.97		
2.77	1.09		
2.92	0.83		
8.69		0.11	0.04
9.56		0.23	0.07

10.44		0.30	0.11
11.32		0.49	0.19
12.19		0.53	0.28
13.07		0.83	0.38
13.94		1.08	0.52
14.82		0.98	0.78
15.69		1.14	0.95
16.57		1.22	1.12
17.45		1.45	1.34
18.32		1.74	1.59
19.20		1.82	1.76
20.07		2.22	1.76
20.95		2.25	2.09
21.82		2.07	2.12

Data of particle velocity in annulus

ABS plastic particle, plastic particle 1, plastic particle 2, $L_d=90\text{cm}$, $H_s=80\text{cm}$, $H_e=0\text{cm}$

Particle density (kg/m^3)	1050	1348	1485
Gas superficial velocity (mm/s)	Particle moving velocity in annulus region (cm/s)		
1.71	0.08		
2.17	0.14		
2.64	0.19		
3.10	0.25		

3.56	0.30		
4.02	0.41		
4.49	0.55		
9.55		0.02	
10.42		0.04	
11.29		0.06	0.02
12.17		0.07	0.03
13.04		0.09	0.04
13.92		0.10	0.06
14.79		0.13	0.07
15.66		0.16	0.09
16.54		0.17	0.12
17.41		0.22	0.16
18.28		0.25	0.18
19.16		0.30	0.20
20.03		0.31	0.23
20.91		0.39	0.28
21.78		0.47	0.31

Data of dense phase retraction in the annulus region

ABS plastic particle, plastic particle 1, plastic particle 2, $L_d=90\text{cm}$, $H_s=80\text{cm}$, $H_e=0\text{cm}$

Particle Density (kg/m^3)	1050		1348		1485	
	Dense phase height(cm)	H_{de}/H_{de0}	Dense phase height(cm)	H_{de}/H_{de0}	Dense phase height(cm)	H_{de}/H_{de0}
1.71	80.0	1.0000				
2.17	80.0	1.0000				
2.64	77.9	0.9740				
3.10	75.7	0.9481				
3.56	74.7	0.9351				
4.02	72.5	0.9091				
4.49	69.4	0.8701				
4.95	67.2	0.8442				
5.41	66.2	0.8312				
5.88	63.0	0.7922				
6.34	60.8	0.7662				
6.80	58.7	0.7403				
7.26	56.6	0.7143				
7.73	55.5	0.7013				
8.19	53.4	0.6753				
8.65	52.3	0.6623				
9.12	49.1	0.6234				
9.55			80.0	1.0000		
10.42			80.0	1.0000		
11.29			79.5	0.9939	80.0	1.0000

12.17			79.5	0.9939	80.0	1.0000
13.04			79.0	0.9877	80.0	1.0000
13.92			79.0	0.9877	80.0	1.0000
14.79			78.6	0.9840	79.5	0.9939
15.66			78.5	0.9816	79.0	0.9878
16.54			78.5	0.9816	78.8	0.9854
17.41			78.3	0.9791	78.5	0.9817
18.28			78.0	0.9755	78.2	0.9780
19.16			77.5	0.9693	78.0	0.9756
20.03			77.0	0.9632	78.0	0.9756
20.91			76.5	0.9571	77.6	0.9707
21.78			75.5	0.9448	77.5	0.9695

Data of dead zone length at wall of column

ABS plastic particle, $H_s=30\text{cm}$, 45cm , 60cm

			Water level(cm)				
	H_s (cm)	Gas flowrate (l/min)	0	3	20	40	60
Average L_n (cm)	30	2	5.50	5.83	6.50	6.50	6.33
		4	4.83	4.67	5.33	6.33	6.83
		8	4.50	4.50	6.00	6.50	
	45	2	6.33	6.33	6.00	6.17	6.17
		4	5.00	5.00	5.17	5.17	5.17
		8	4.17	4.17	4.17	4.33	4.17
	60	2	6.33	6.67	6.50	6.50	6.67
		4	4.83	4.33	4.33	4.50	4.50
		8	4.50	4.17	4.33	4.33	4.17

Curriculum Vitae

Name: Jia Meng

Post-secondary Education and Degrees: University of Western Ontario
London, Ontario, Canada
2017-2018 M.ESc

Tianjin University
Tianjin, Tianjin, China
2013-2017 B.Eng

Related Work Experience: Teaching Assistant
University of Western Ontario
2017-2018

Research Assistant
The University of Western Ontario
2017-2018